Quantum Anomalous Hall Effect and Quantum Hall Effect in Topological Insulator Thin Film

沈顺清
Shun-Qing Shen

Department of Physics

香 港 大 學
THE UNIVERSITY OF HONG KONG

Hall Effect

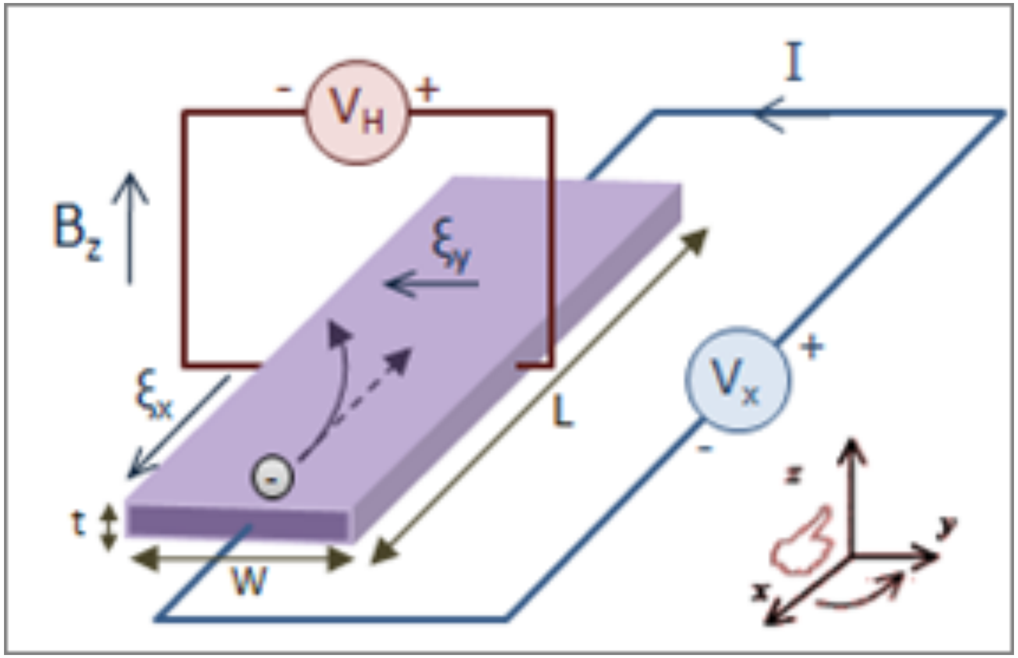

Lorentz force:

$$F = q(v \times B + E)$$

$$V_H = -\frac{IB}{\rho_e q t}$$

$$\rho_H = -\frac{B}{q\rho_e}$$

Hall Coefficient: $R_H = -\dfrac{1}{q\rho_e}$

Application:

1. To measure the sign of charge carriers
2. To measure the density of the charge density
3. To measure the magnetic field

Anomalous Hall Effect

In a ferromagnetic metal,

$$\rho_H = R_H B + R_A M$$

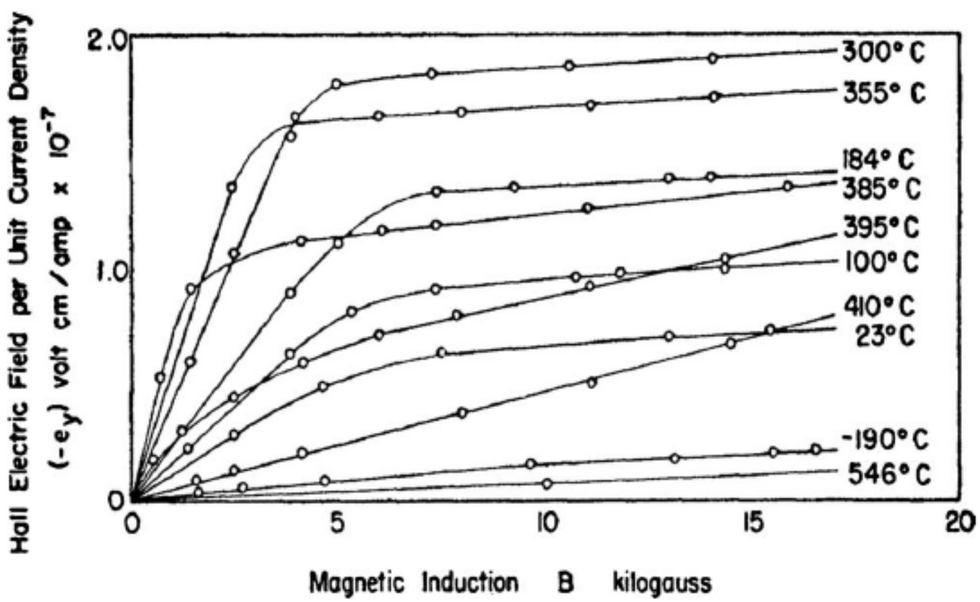

FIG. 1. The Hall effect in Ni (data from Smith, 1910). From Pugh and Rostoker, 1953.

Integer Quantum Hall Effect & Edge States

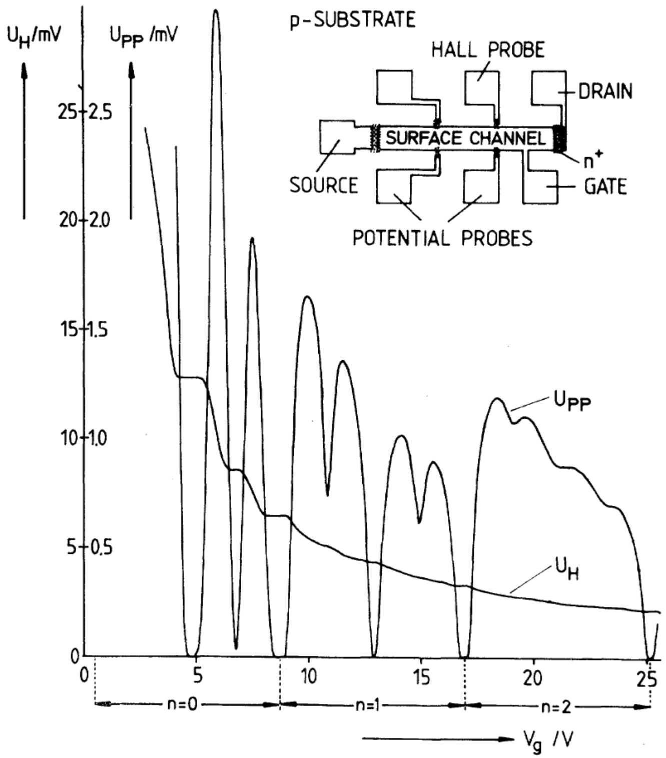

Klitzing, K. von; Dorda, G.; Pepper, M. "New Method for High-Accuracy Determination of the Fine-Structure Constant Based on Quantized Hall Resistance". *Phys. Rev. Lett.* **45** (6): 494–497 (1980).

$$\rho_{xy} = -\frac{\sigma_{xy}}{\sigma_{xx}^2 + \sigma_{xy}^2} = -\sigma_{xy}^{-1} = -\frac{h}{ne^2}$$

n is an integer.

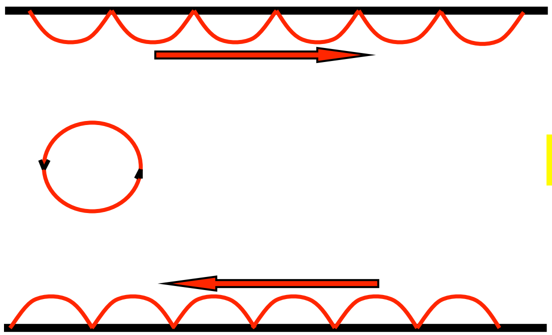

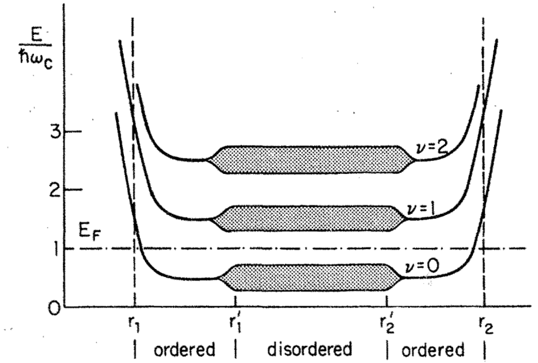

$k_x \to y_0 / l_b^2$

$$i_n = -\frac{e}{L}\sum \langle v_x \rangle_n = -\frac{e}{L}\sum_{k_x} \langle \partial H / \hbar \partial k_x \rangle_n$$
$$= -\frac{e}{2\pi\hbar}\int dk_x \frac{\partial E_n}{\partial k_x} \to -\frac{e}{h}\int dy_0 \frac{\partial E_n}{\partial y_0}$$
$$= -\frac{e}{h}\left[E_n(L/2) - E_n(-L/2)\right]$$
$$= \frac{e^2}{h} V$$

Halperin, 82; Streda & MacDonald, 84

The key feature:
Bulk electrons are localized
while edge electrons are extended.

A free electron in a B field

$$H = \frac{1}{2m}\left(\mathbf{p} - e\mathbf{A}\right)^2$$

$$B = \partial_x A_y - \partial_y A_x \quad A_x = -By, A_y = 0$$

$$H = -\frac{\hbar^2}{2m}\partial_y^2 + \frac{e^2B^2}{2m}(y - y_0)^2$$

$$y_0 = -\frac{\hbar k_x}{eB}$$

$$E_n = \hbar\omega(n + 1/2)$$

$$\phi_n(-x) = (-1)^n\phi(x)$$

Edge state of a rigid wall

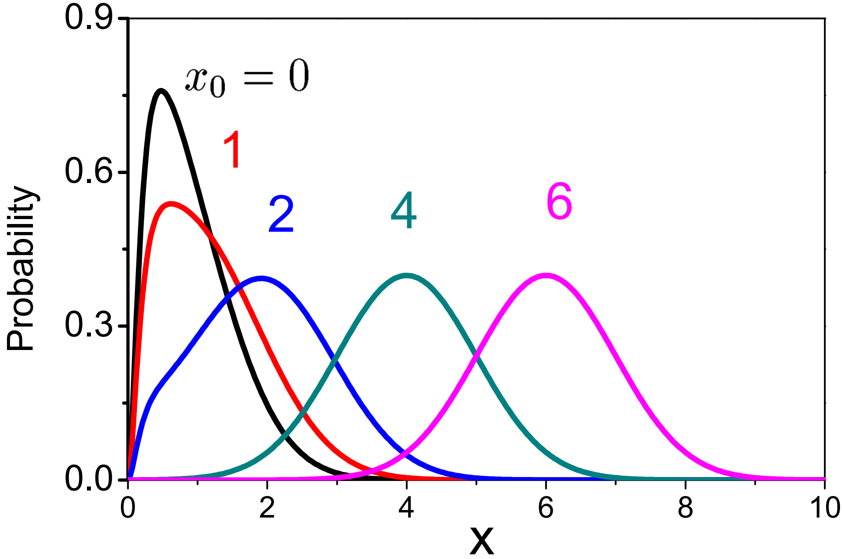

$$i_n = -\frac{e}{L}\sum \langle v_x \rangle_n = -\frac{e}{L}\sum_{k_x} \langle \partial H / \hbar \partial k_x \rangle_n$$

$$= -\frac{e}{2\pi\hbar}\int dk_x \frac{\partial E_n}{\partial k_x} \to -\frac{e}{h}\int dy_0 \frac{\partial E_n}{\partial y_0}$$

$$= -\frac{e}{h}\left[E_n(L/2) - E_n(-L/2)\right]$$

$$= \frac{e^2}{h}V$$

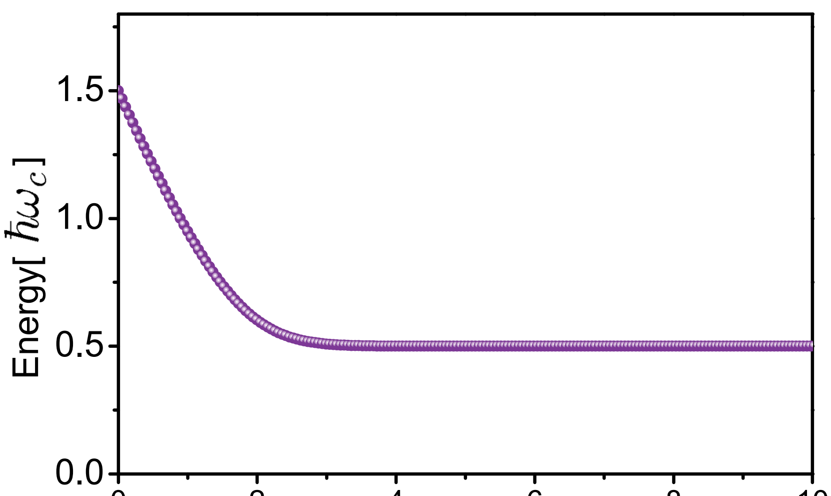

$$v_x = \frac{\partial E}{\hbar \partial k_x} = -\frac{1}{eB}\frac{\partial E}{\partial y_0}$$

3D Topological Insulator

Under the time reversal

$$\Theta H(k)\Theta^{-1} = H(-k)$$

Time Reversal Invariant Momentum

$$k = -k + G; \quad k = G/2$$

(Reciprocal lattice vector G)

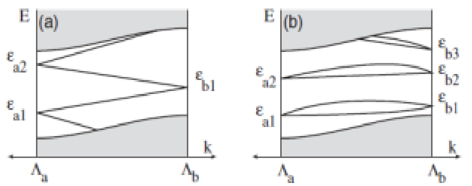

FIG. 1. Schematic surface (or edge) state spectra as a function of momentum along a line connecting Λ_a to Λ_b for (a) $\pi_a\pi_b = -1$ and (b) $\pi_a\pi_b = +1$. The shaded region shows the bulk states. In (a) the TRP changes between Λ_a and Λ_b, while in (b) it does not.

Fu and Kane, PRL 98, 106803 (2007)

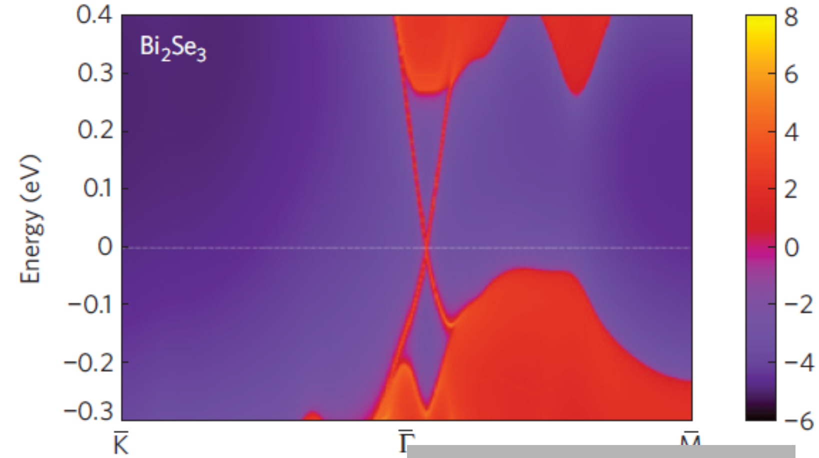

Zhang et al, Nat. Phys (2009)

The surface states in the gap:
1.The Fermi surface encloses an odd number of Dirac cones;
2.The Fermi surface has a single spin state at each momentum, the lock-in relation of electron momentum and spin;
3.The Berry phase arround the Fermi surface is π.

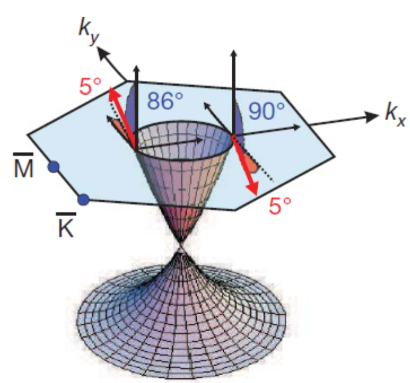

Hsieh et al, Nature (2009)

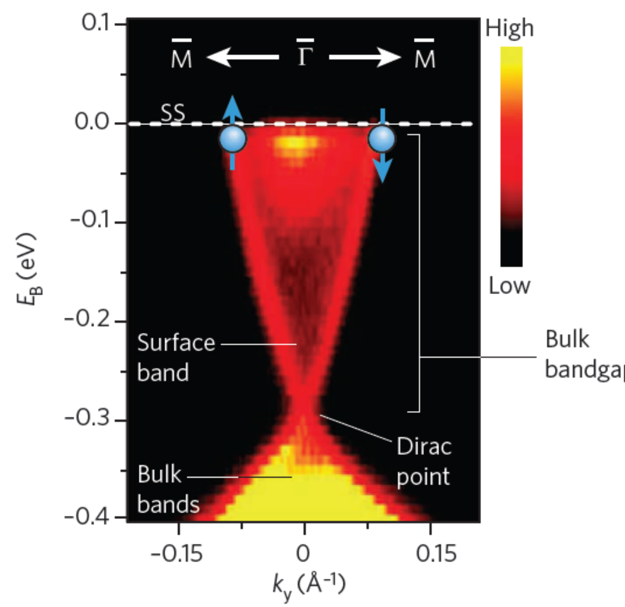

Xia et al, Nat. Phys, (2009)

Topological insulators in Bi_2Se_3, Bi_2Te_3 and Sb_2Te_3 with a single Dirac cone on the surface

Haijun Zhang[1], Chao-Xing Liu[2], Xiao-Liang Qi[3], Xi Dai[1], Zhong Fang[1] and Shou-Cheng Zhang[3]★

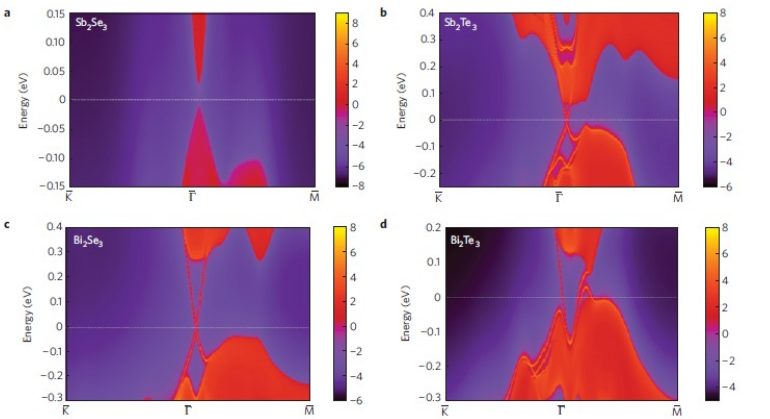

Figure 4 | Surface states. a–d, Energy and momentum dependence of the LDOS for Sb_2Se_3 (**a**), Sb_2Te_3 (**b**), Bi_2Se_3 (**c**) and Bi_2Te_3 (**d**) on the [111] surface. Here, the warmer colours represent higher LDOS. The red regions indicate bulk energy bands and the blue regions indicate bulk energy gaps. The surface states can be clearly seen around the Γ point as red lines dispersing in the bulk gap for Sb_2Te_3, Bi_2Se_3 and Bi_2Te_3. No surface state exists for Sb_2Se_3.

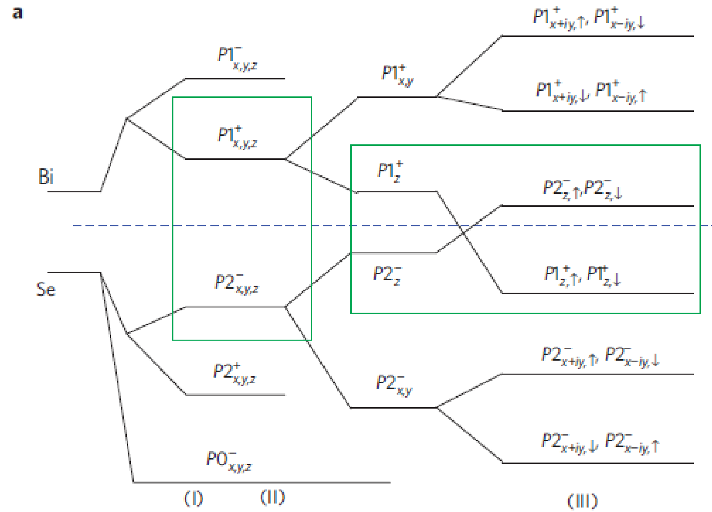

$$H(k) = (C - D_1\partial_z^2 + D_2k^2) + \begin{pmatrix} h(A_1) & A_2k_-\sigma_x \\ A_2k_+\sigma_x & h(-A_1) \end{pmatrix}$$

$$h(A_1) = (M + B_1\partial_z^2 - B_2k^2)\sigma_z - iA_1\partial_z\sigma_x$$

$$k_\pm = k_x \pm ik_y, k^2 = k_x^2 + k_y^2$$

Surface states:

Shan, Lu & Shen, NJP(2010)

$$H_{eff} = \varepsilon_0 - Dk^2 + v_F\hbar(k_x\sigma_x + k_y\sigma_y)$$

$$\hbar v_F = \sqrt{1 - D_1^2 / B_1^2}A_2$$

From 3D to 2D

Consider an ultrathin film with thickness L. The open boundary conditions are taken at the surface $\Psi(z = \pm L/2) = 0$

Method I: The problem can be solved exactly. $\Psi(z) \propto (e^{-\lambda_1 z} - e^{-\lambda_2 z})$

Method II: Solve the 3D equation at $k_x = k_y = 0$

The four solutions of the surface states are obtained for four p electrons, which can be used as the new basis to expand the 3D model around the point, $k_x = k_y = 0$

$$H_{\text{eff}} = \begin{bmatrix} h_+(k) & 0 \\ 0 & h_-(k) \end{bmatrix}$$

$$h_{\tau_z}(k) = E_0 - Dk^2 - v_F \hbar (k_x \sigma_y - k_y \sigma_x) + \tau_z \left(\frac{\Delta}{2} - Bk^2\right)\sigma_z$$

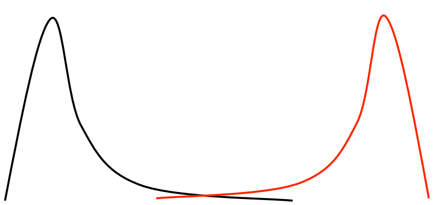

Energy Gap Δ

Lu et al, 2010
Shan et al, 2010

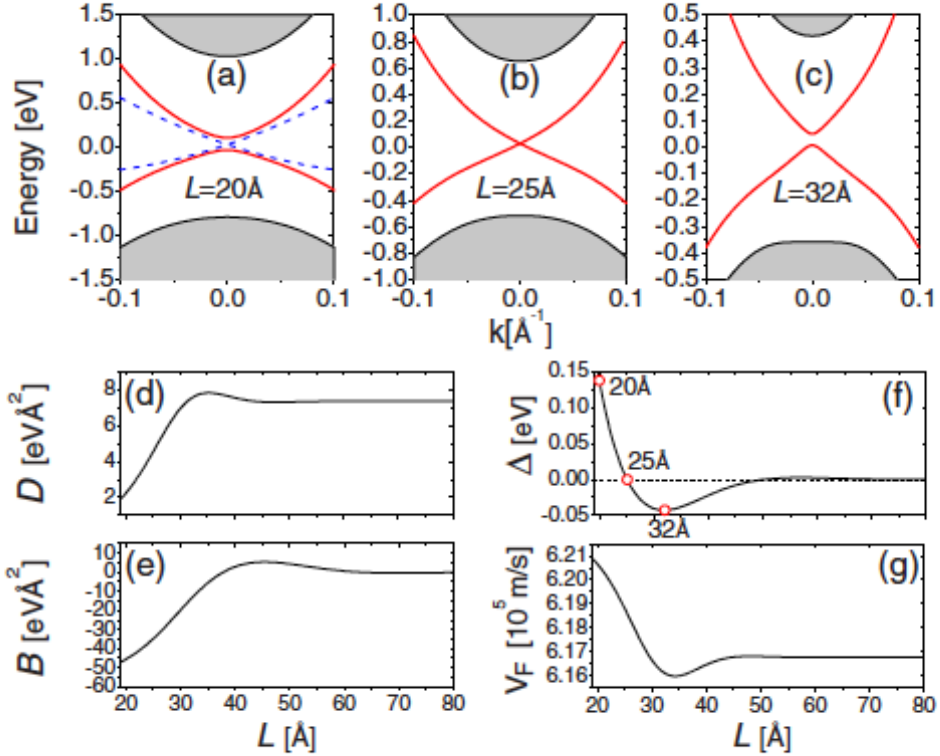

FIG. 2. (Color online) [(a)–(c)] Twofold degenerate ($\tau_z = \pm 1$) energy spectra of surface states for thicknesses $L = 20, 25, 32$ Å (solid lines), and $L \to \infty$ (dash lines). The gray area corresponds to the bulk states. The energy spectra are obtained by solving $H(k, -i\partial_z)\Psi(z) = E\Psi(z)$ under the boundary conditions $\Psi(z = \pm L/2) = 0$. Please note that the scales of energy axis in (a)–(c) are different. The model parameters are adopted from Ref. 9: $M = 0.28$ eV, $A_1 = 2.2$ eV Å, $A_2 = 4.1$ eV Å, $B_1 = 10$ eV Å^2, $B_2 = 56.6$ eV Å^2, $C = -0.0068$ eV, $D_1 = 1.3$ eV Å^2, and $D_2 = 19.6$ eV Å^2. [(d)–(g)] The parameters for the new effective model H_{eff}: D, B, the energy gap Δ, and the Fermi velocity v_F vs L.

Structural Inversion Asymmetry and Effective Hamiltonian

Introduce an asymmetric potential along the z direction. Because of the substrate the two boundary conditions of the wave function at the two surfaces are different.

$$V(z) = V(-z)$$

$$V_{eff} = \int dz \Psi^{+}(z) V(z) \Psi(z) = \begin{pmatrix} & & V_0 & 0 \\ & & 0 & V_0^{*} \\ V_0^{*} & 0 & & \\ 0 & V_0 & & \end{pmatrix}$$

For example

$$V(z) = -Ez$$

$$V(z) = \begin{cases} +V & 0 < z < L/2 \\ -V & -L/2 < 0 \end{cases}$$

Bi_2Se_3 Thin Films

Zhang et al, Nat. Phys. 6, 584 (2010)

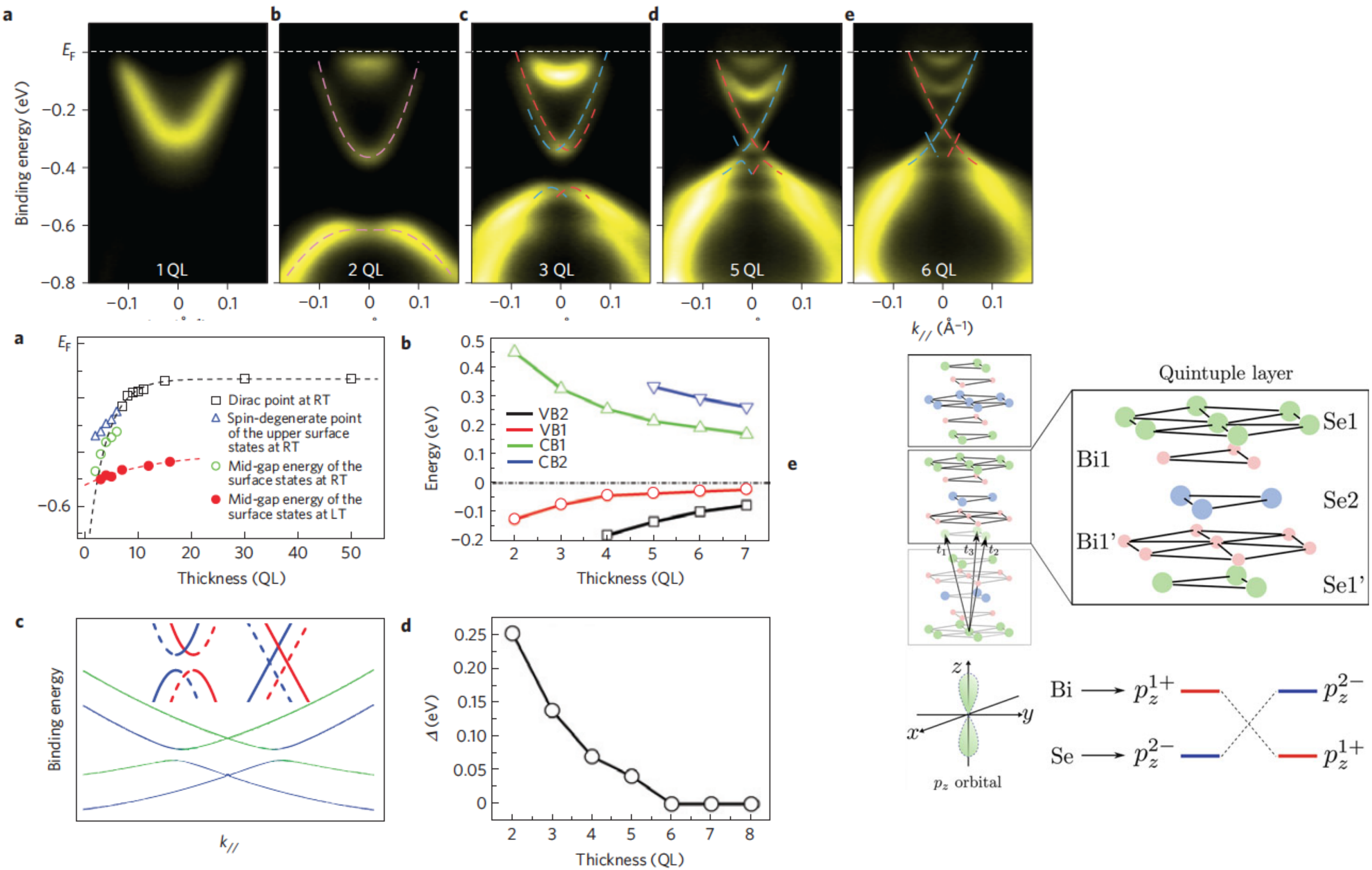

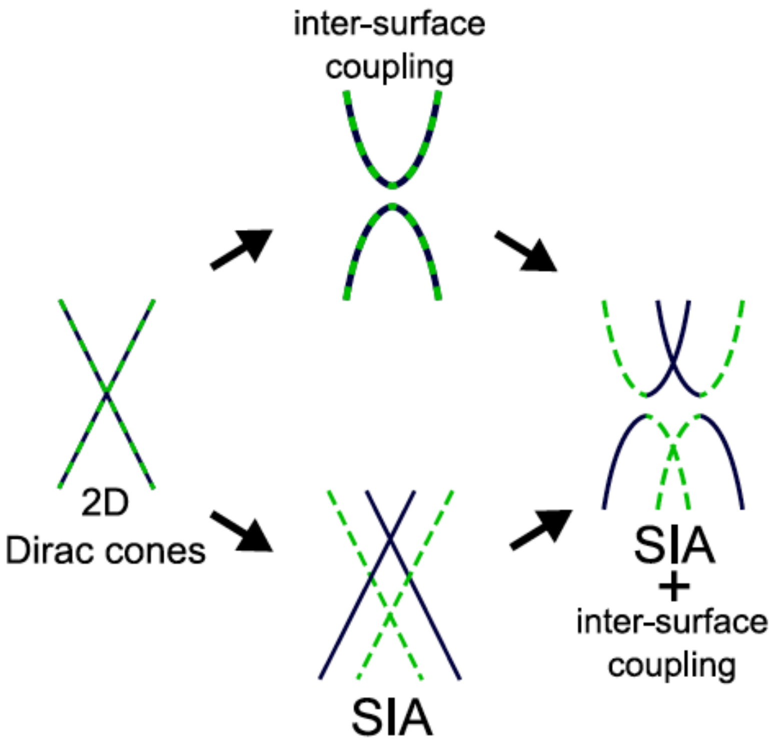

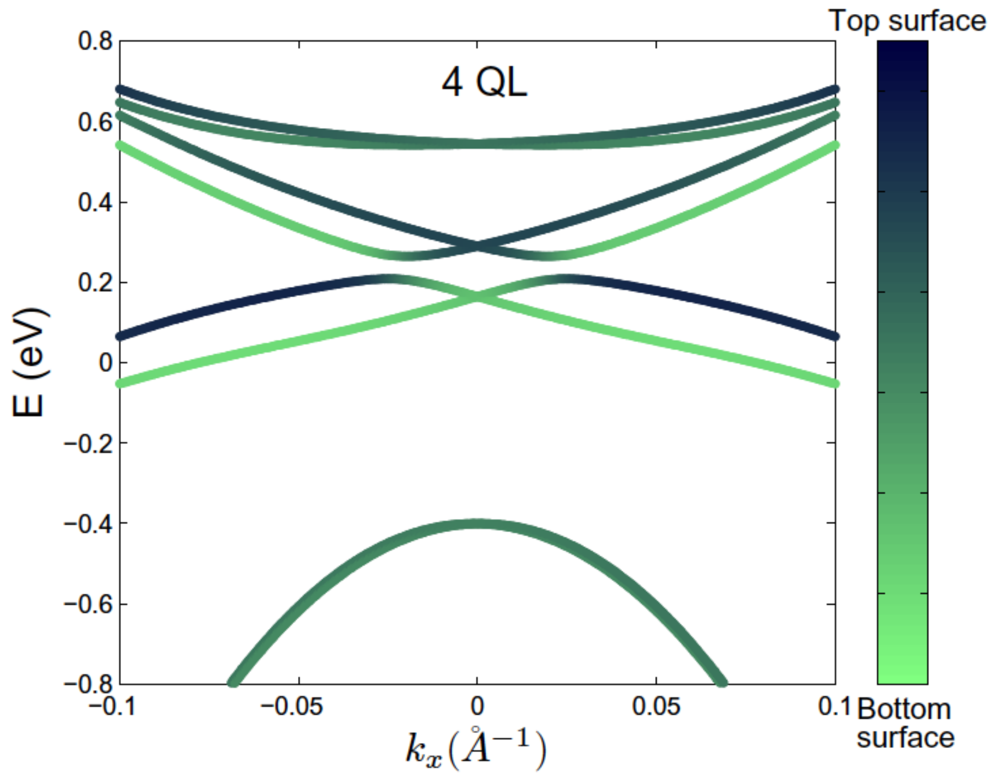

Evolution of surface states
In a thin film

Shan, Lu, and Shen, New J Phys, (2010)

Microscopic Model for TI Thin Film

$$H_0 = -Dk^2 + \begin{pmatrix} \frac{\Delta}{2} - Bk^2 & i\gamma k_- & V & 0 \\ -i\gamma k_+ & -\frac{\Delta}{2} + Bk^2 & 0 & V \\ V & 0 & -\frac{\Delta}{2} + Bk^2 & i\gamma k_- \\ 0 & V & -i\gamma k_+ & \frac{\Delta}{2} - Bk^2 \end{pmatrix}$$

Table 1 | Parameters of equations (1) and (2) used to fit the bands in Fig. 2b–e, and the fitted Rashba parameters (α_R).

QL	E_0(eV)	D (eV Å^2)	Δ (eV)	B (eV Å^2)	v_F (10^5 m s^{-1})	$\lvert\tilde{V}'\rvert$ (eV)	α_R (eV Å)
2	−0.470	−14.4	0.252	21.8	4.71	0	0
3	−0.407	−9.7	0.138	18.0	4.81	0.038	0.71
4	−0.363	−8.0	0.070	10.0	4.48	0.053	1.27
5	−0.345	−15.3	0.041	5.0	4.53	0.057	2.42
6	−0.324	−13.0	0	0	4.52	0.068	2.78

Zhang et al, Nat. Phys, (2010)

Two Insulating Phases: Band Gap Insulator and QSHE

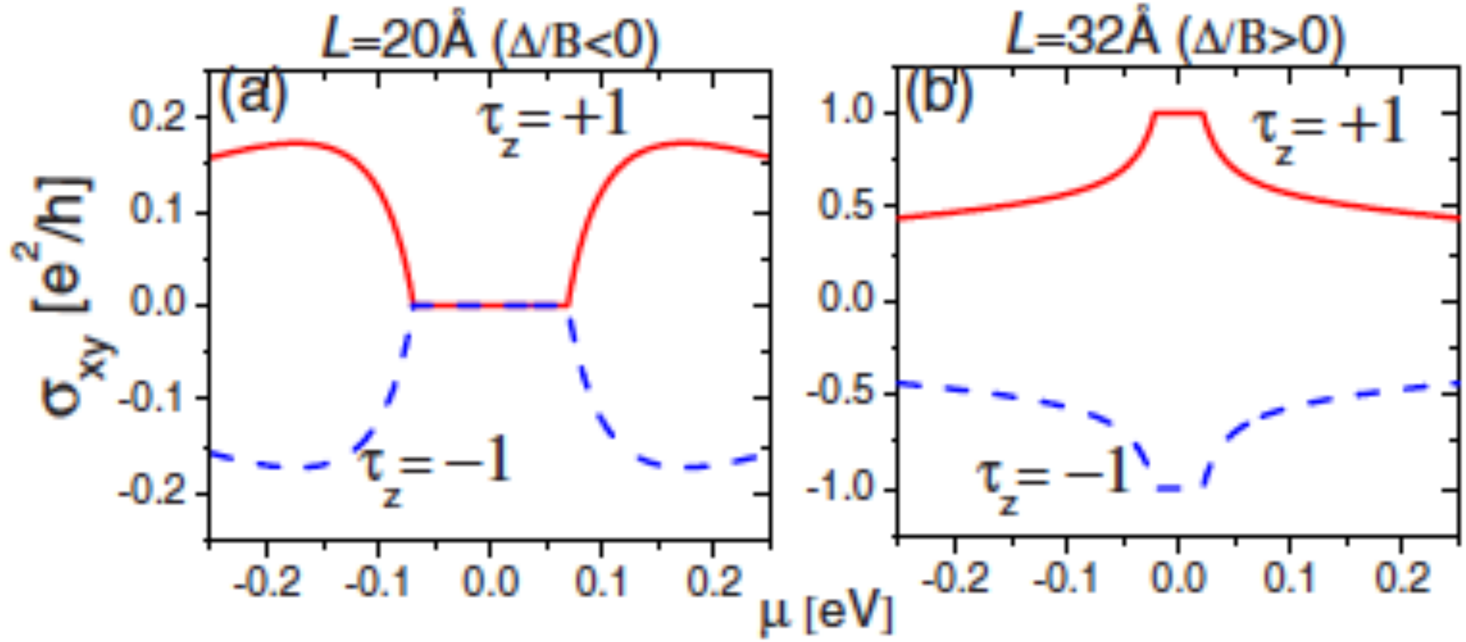

FIG. 5. (Color online) The hyperbola-dependent Hall conductance vs Fermi level μ for (a) L=20 Å and (b) 32 Å, respectively.

In the absence of SIA.

Magnetic doping

Doping magnetic impurities (Hor et al, PRB 08; Chen, ZXShen et al, Science 10; Wray, Hasan et al Nat. Phys. 11):

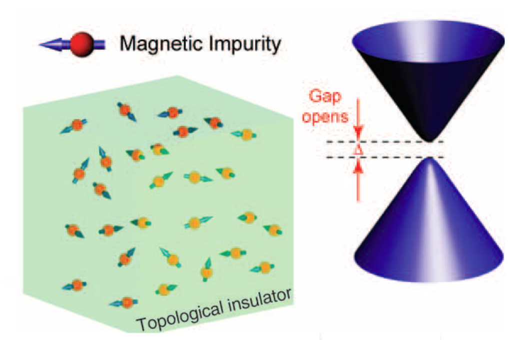

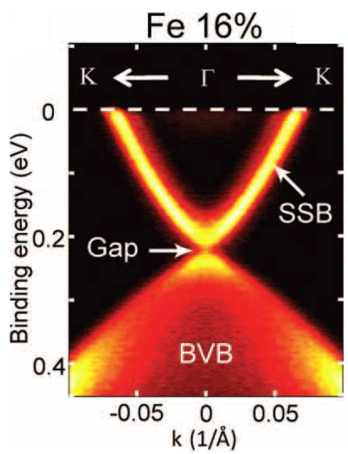

Chen, ZXShen et al, Science, 10

When ferromagnetic order is formed, the z-component magnetization can open a gap at Dirac point

QAHE in Fe- or Cr-doped tetradymite semiconductor Bi_2Te_3 and Bi_2Se_3

Yu et al, Science 329, 61 (2010).

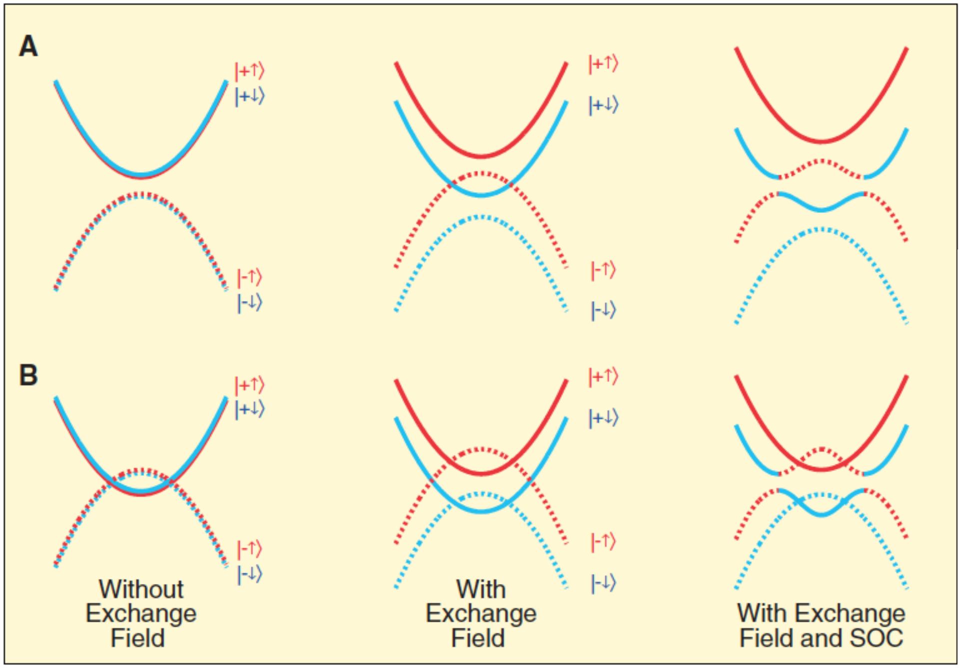

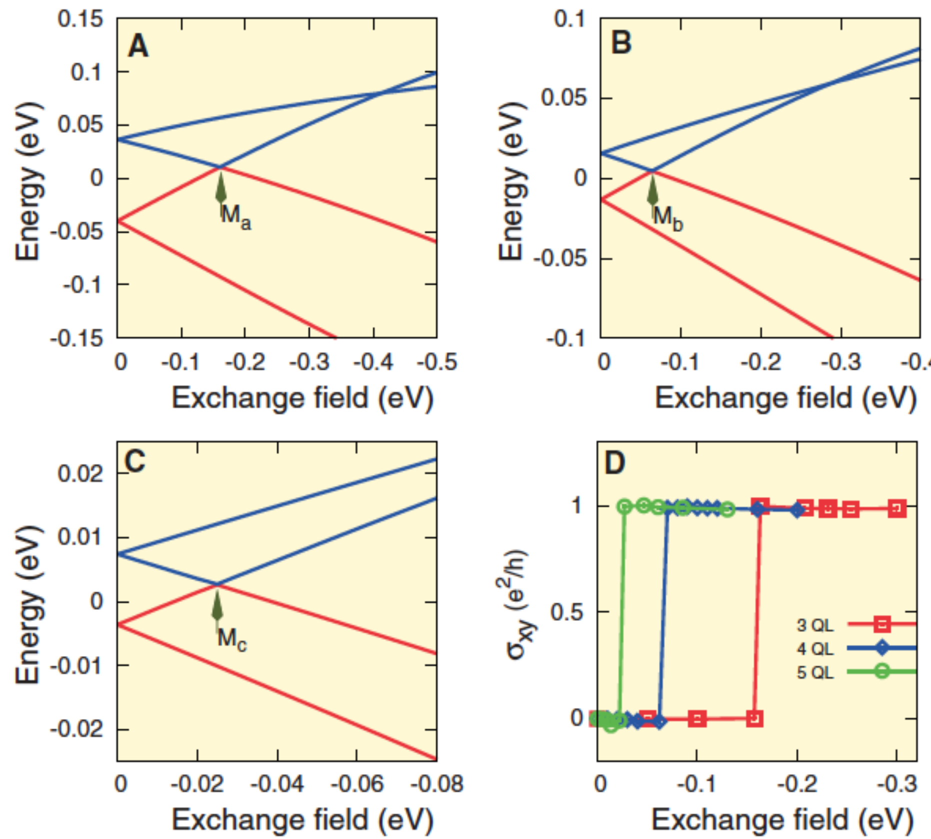

Experimental Observation of QAHE

Chang et al, Science (2013)

Sample: Cr-doped (Bi,Sb)2Te3 thin film

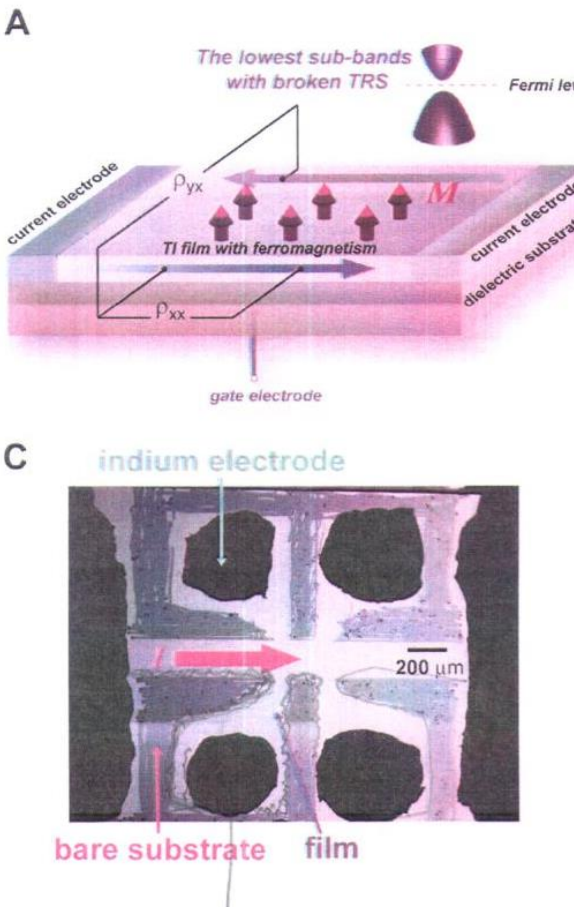

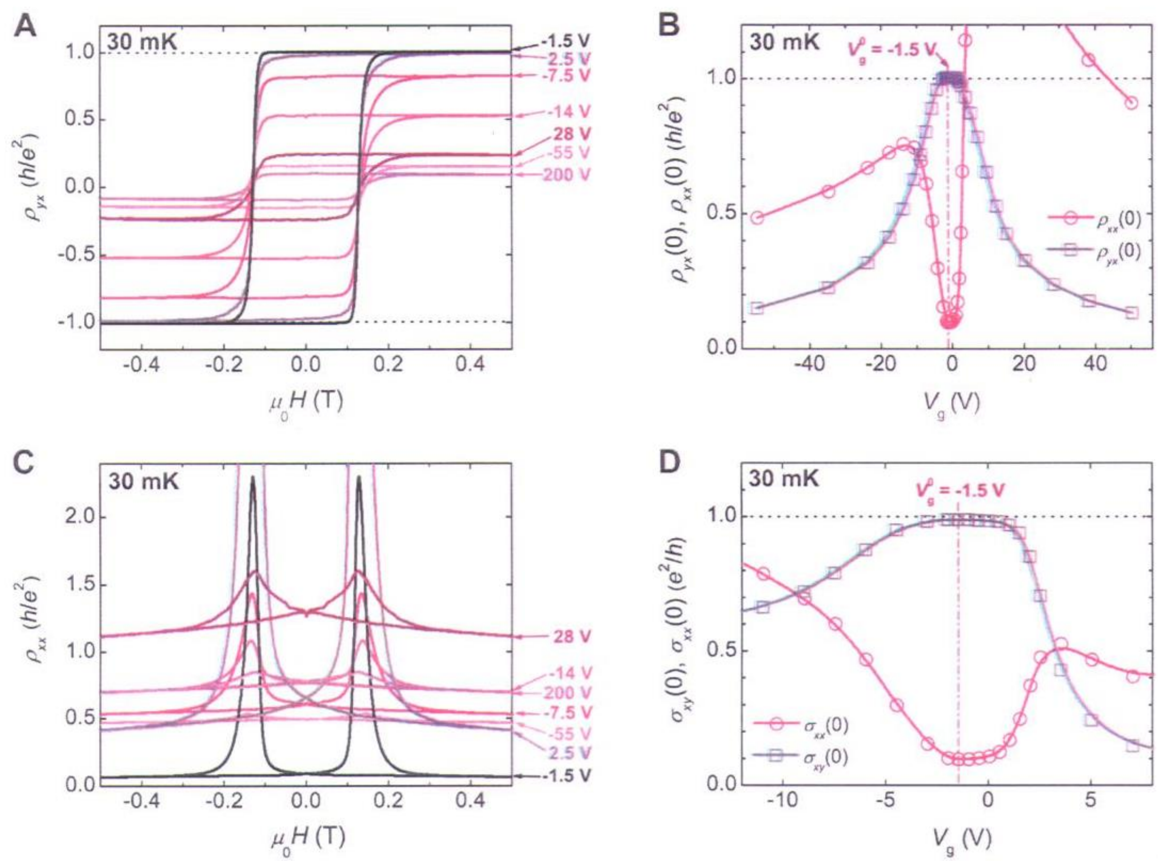

Exchange Field

$$H = H_0 + \frac{m}{2}\tau_0 \otimes \sigma_z .$$

Yu et al, 2010

$$H = -Dk^2 + \begin{pmatrix} \frac{\Delta + m}{2} - Bk^2 & i\gamma k_- & V & 0 \\ -i\gamma k_+ & -\frac{\Delta + m}{2} - Bk^2 & 0 & V \\ V & 0 & -\frac{\Delta - m}{2} - Bk^2 & i\gamma k_- \\ 0 & V & -i\gamma k_+ & \frac{\Delta - m}{2} - Bk^2 \end{pmatrix}$$

Band Structure

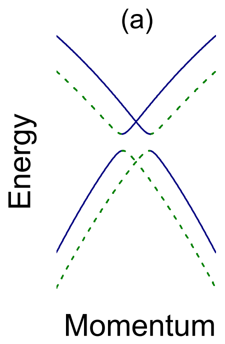

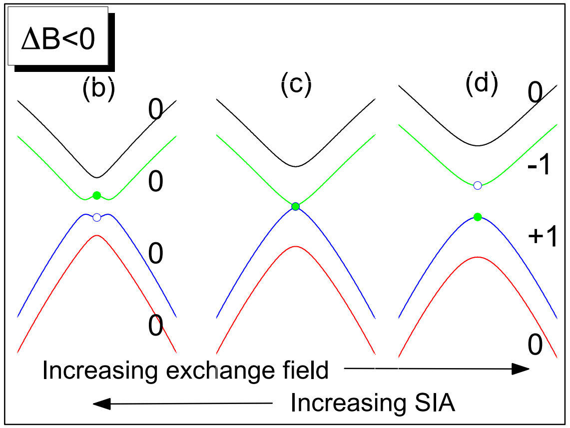

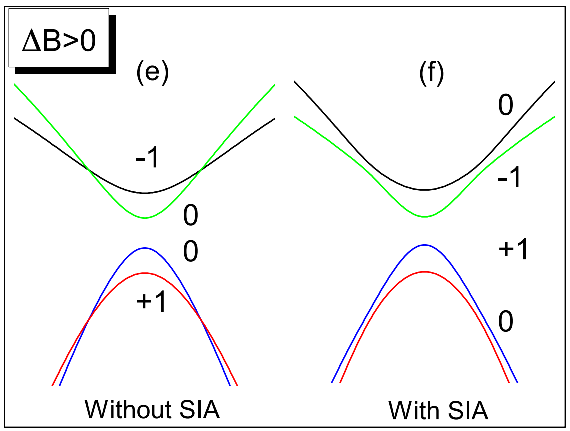

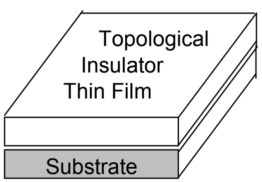

Under a unitary transformation, the 4X4 matrix can be reduced into two 2X2 matrcies

$$h_s = -Dk^2 + \sigma_z (\Gamma + s\Lambda) + s\gamma(k_x\sigma_y - k_y\sigma_x)\cos\Theta$$

where $s = \pm 1$ for the outer and inner blocks

$$\Gamma = \sqrt{(m/2)^2 + \gamma^2 k^2 \sin^2\Theta}$$
$$\Lambda = \sqrt{(\Delta/2 - Bk^2)^2 + V^2},$$
$$\cos\Theta = (\Delta/2 - Bk^2)/\Lambda$$

A transition occurs at $\Gamma = \Lambda$

The condition for QAHE: $|m| > \sqrt{\Delta^2 + 4V^2}$

Longitudinal & Transverse Conductance

Berry curvature and the Hall conductance

$$\Omega_i^z(\mathbf{k}) = -2\sum_{j\neq i}\frac{\mathrm{Im}\langle i|\partial H/\partial k_x|j\rangle\langle j|\partial H/\partial k_y|i\rangle}{(E_i-E_j)^2}$$

$$\sigma_{xy} = -\frac{e^2}{h}\sum_i\int\frac{d^2\mathbf{k}}{(2\pi)^2}f(E_i-E_F)\Omega_i^z(\mathbf{k})$$

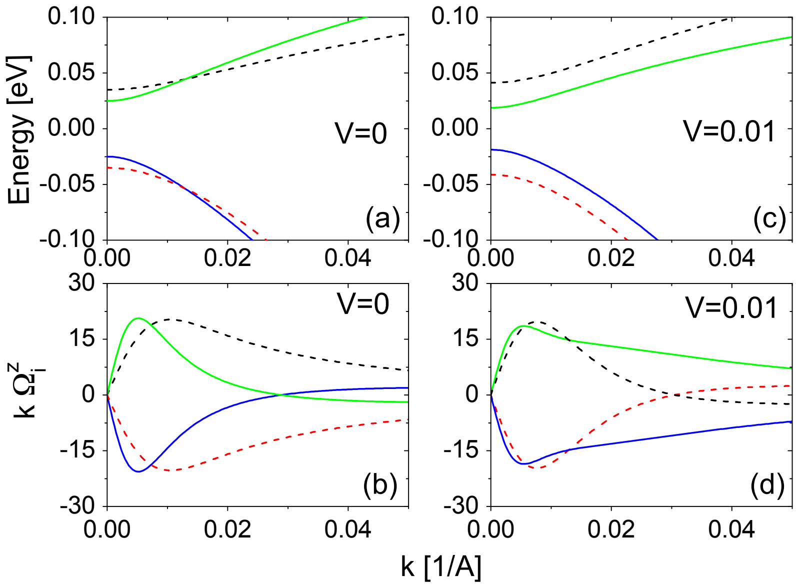

Longitudinal conductance

Using the Einstein relation, $\sigma_{xx} = e^2 N_F \breve{D}$

the diffusion coefficient $\breve{D} = v_F^2\tau/2$

the scattering time $\tau = \hbar/(2\pi N_F n u^2)$

$$\boxed{\sigma_{xx} = \frac{e^2}{h}\sum_{i=1}^{4}\frac{1}{2}\left|\frac{\partial E_i}{\partial k}\right|^2_{E_i=E_F}\frac{1}{nu_i^2}}$$

Comparing with experimental data

Lu, Zhao and Shen, PRL 111, 146802 (2013)

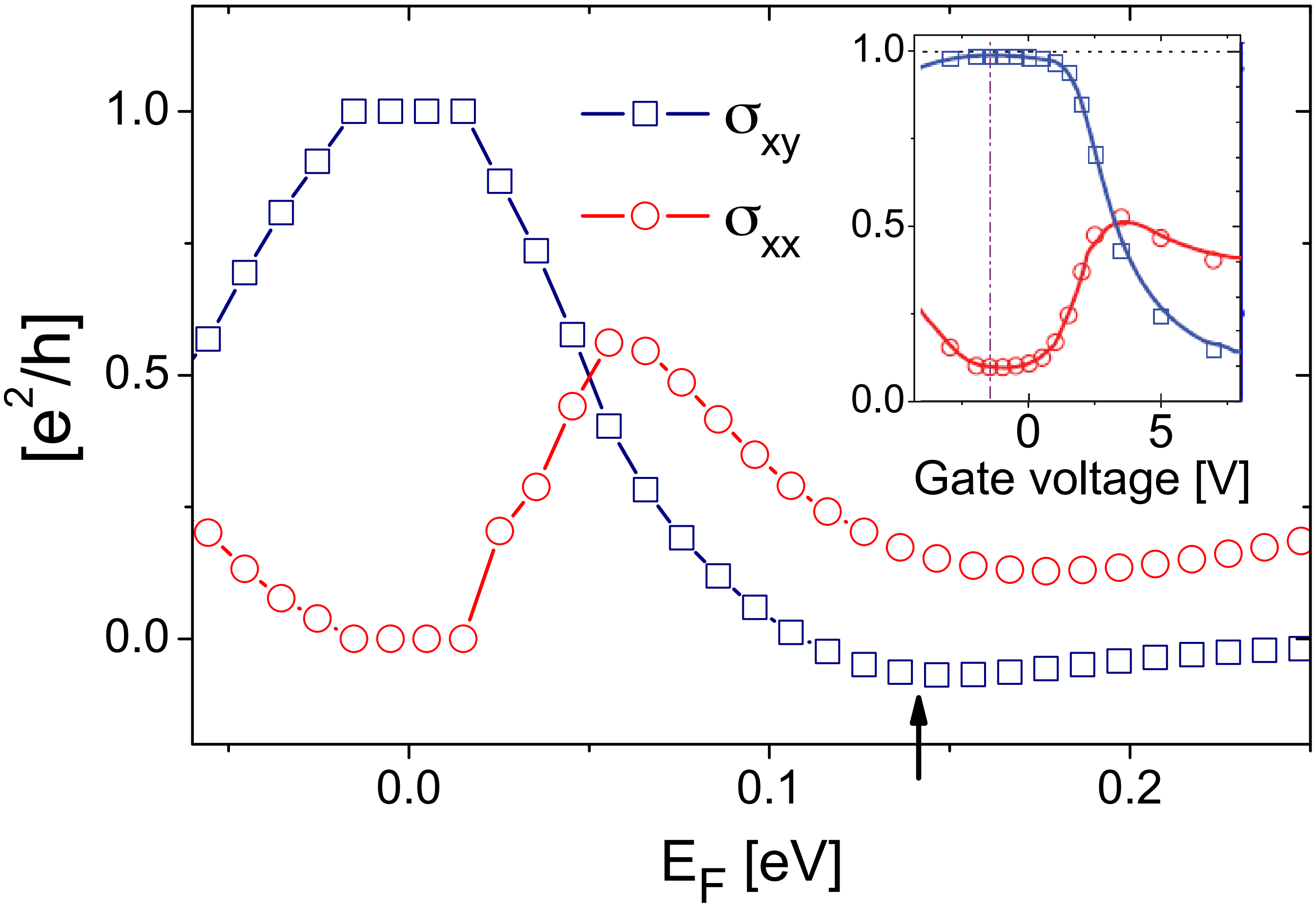

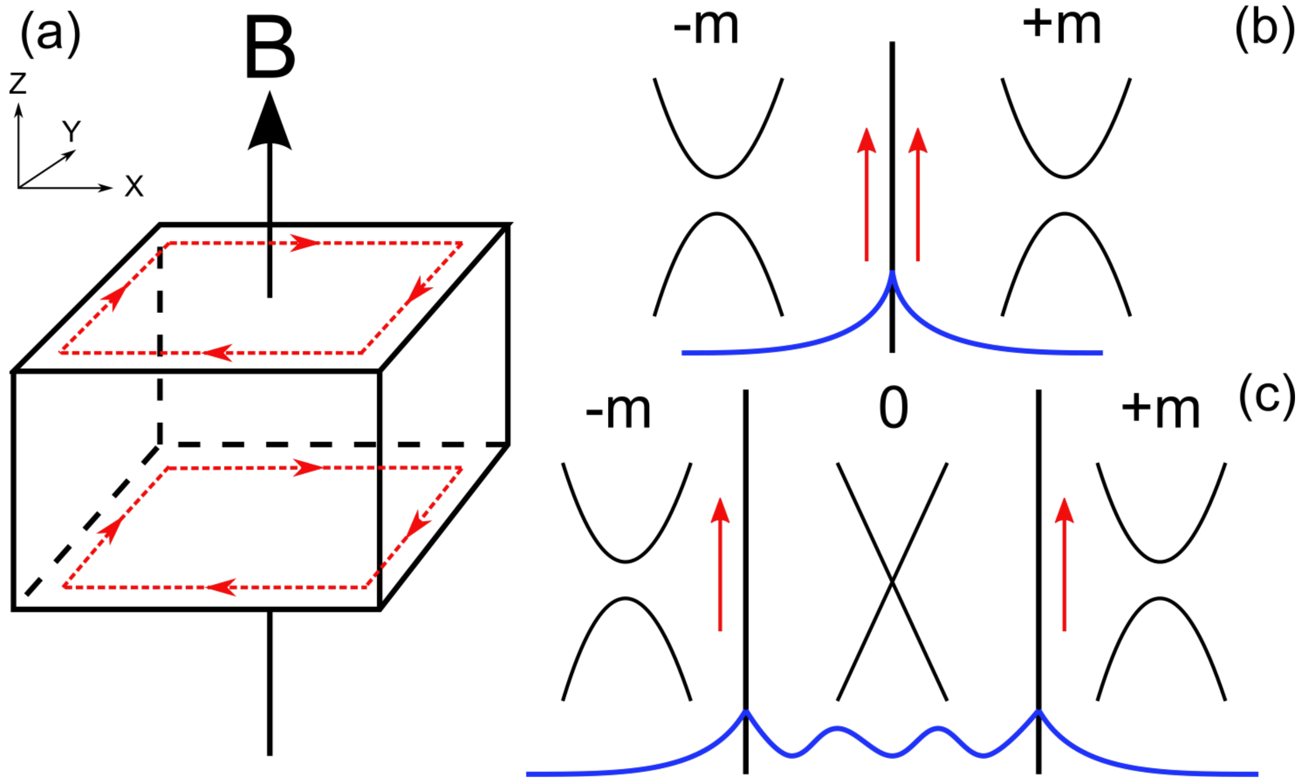

FIG. 1. (Color online) (a) Schematic of a 3D TI in a weak Zeeman field, and the formation of chiral current on the top and bottom surface boundaries. (b) A chiral edge state will form around the domain wall between the 2D Dirac fermions with positive and negative masses, and the wave function is illustrated. The arrow indicates the flow of edge current. (c) When the sharp domain wall evolves to finite-width metallic band, the edge mode is effectively split to two halves concentrated around the two bound[aries.]

Chu, Shi, and Shen, PRB 84, 085312 (2011)

Thickness Dependence of the Difference

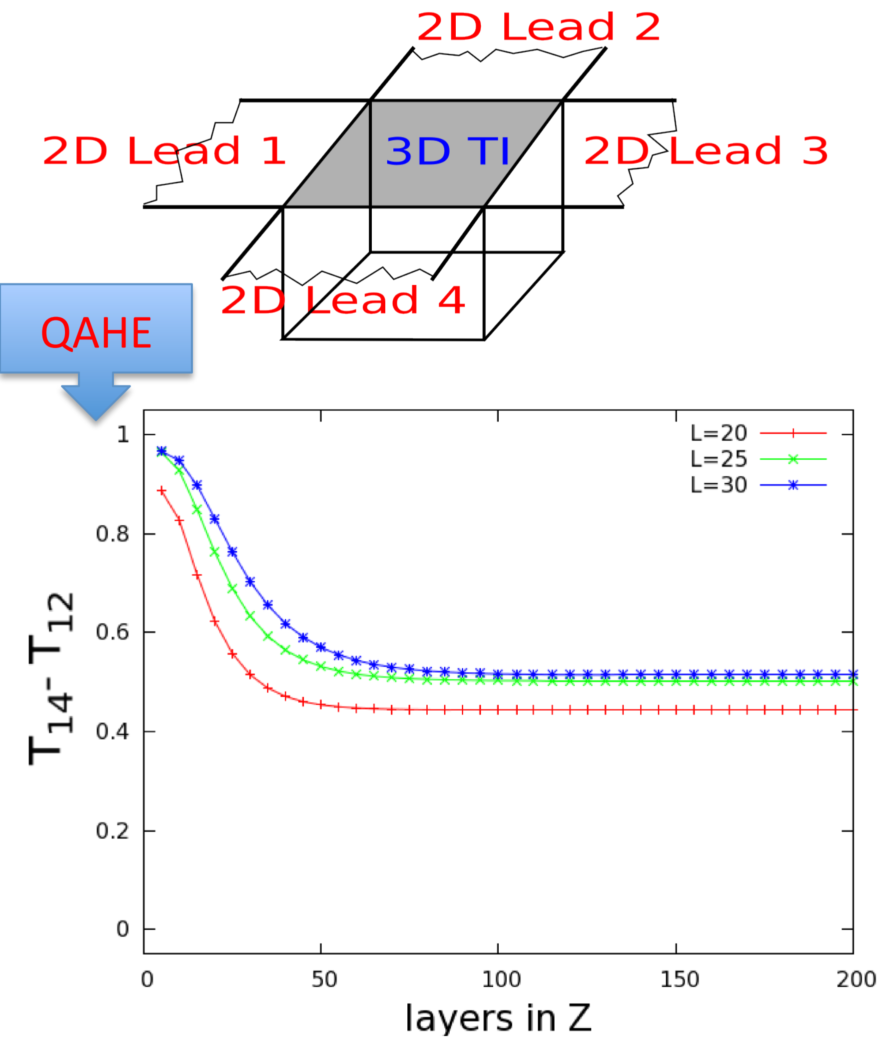

(upper) Schematic illustration of the 3D device with 2D semi-infinite metallic leads, the sample has finite thickness in Z direction, the top surface size is L×L; (lower) Transmission coefficients $T_{14} - T_{12}$ of the 4-terminal device as a function of the sample thickness in Z. $\Delta z = 0.15$, $M = 0.4$, $E_{f1} = 0.001$, $E_{f2} = 0.04$.

Observation of topological surface state quantum Hall effect in an intrinsic three-dimensional topological insulator

Nature Phys. 10, 956 (2014)

Yang Xu[1,2], Ireneusz Miotkowski[1], Chang Liu[3,4], Jifa Tian[1,2], Hyoungdo Nam[5], Nasser Alidoust[3,4], Jiuning Hu[2,6], Chih-Kang Shih[5], M. Zahid Hasan[3,4] and Yong P. Chen[1,2,6★]

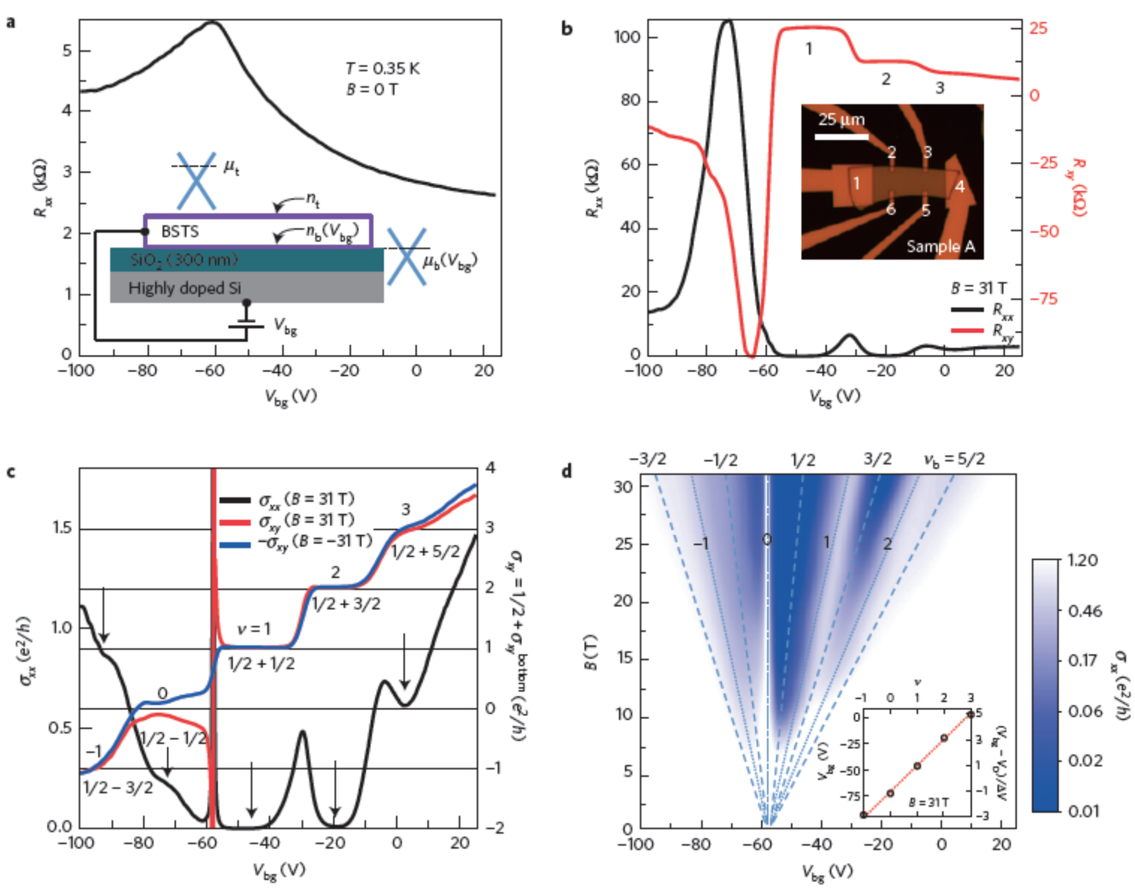

Quantum Hall effect on top and bottom surface states of topological insulator $(Bi_{1-x}Sb_x)_2Te_3$ films

R. Yoshimi[1], A. Tsukazaki[2,3], Y. Kozuka[1], J. Falson[1], K.S. Takahashi[4], J.G. Checkelsky[1,†], N. Nagaosa[1,4], M. Kawasaki[1,4] & Y. Tokura[1,4]

DOI: 10.1038/ncomms7627

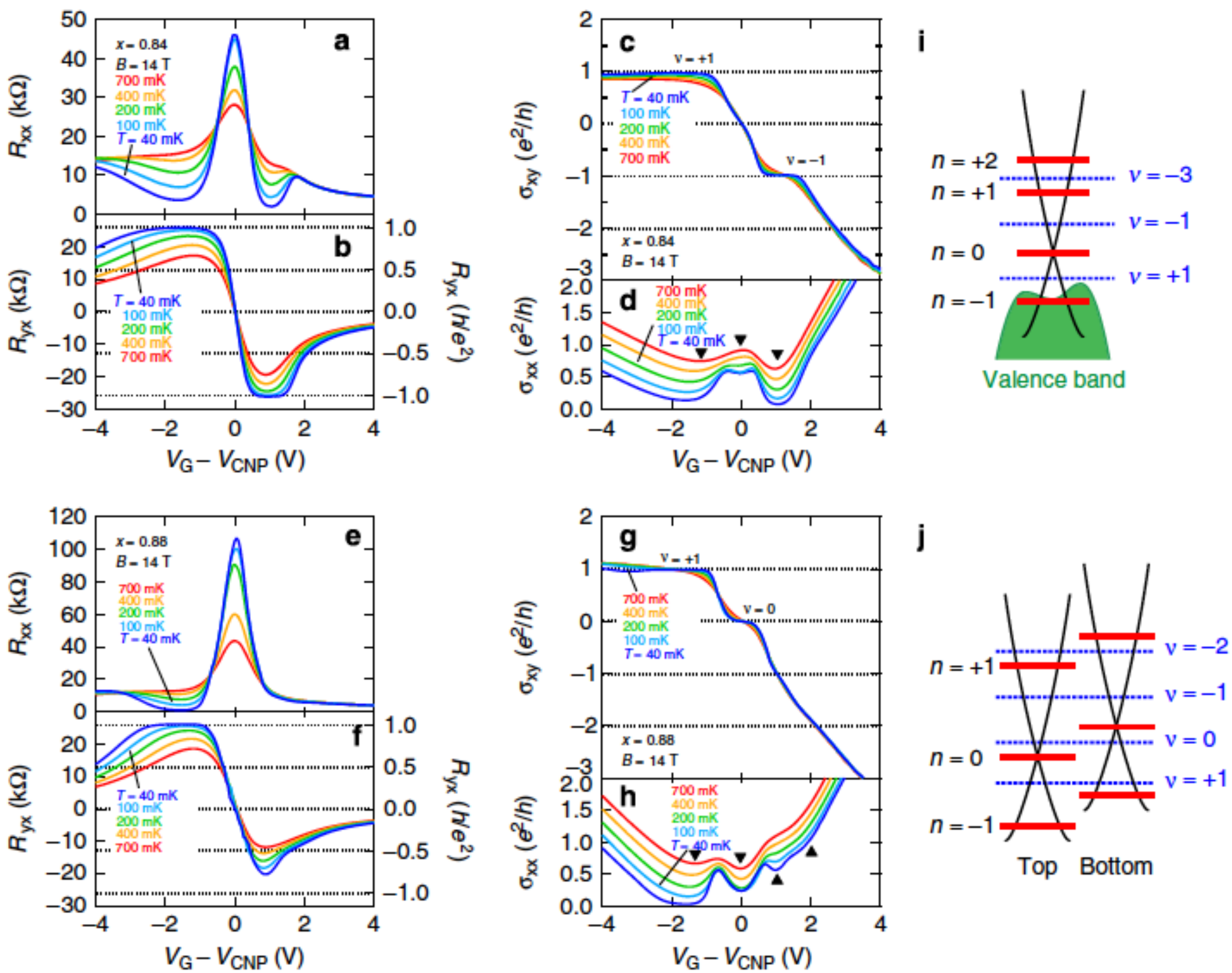

Solutions of an electron in TI thin film in the presence of a uniform B field

Zhang, Lu and Shen, Sci. Rep. (2015)/arXiv: 1502.01792

$$H_0 = \begin{pmatrix} \frac{\Delta}{2} - \omega_+\left(\frac{\xi^2}{4} - \partial_\xi^2\right) & -i\eta\left(\partial_\xi + \frac{\xi}{2}\right) & V & 0 \\ -i\eta\left(\partial_\xi - \frac{\xi}{2}\right) & -\frac{\Delta}{2} - \omega_-\left(\frac{\xi^2}{4} - \partial_\xi^2\right) & 0 & V \\ V & 0 & -\frac{\Delta}{2} - \omega_-\left(\frac{\xi^2}{4} - \partial_\xi^2\right) & -i\eta\left(\partial_\xi + \frac{\xi}{2}\right) \\ 0 & V & -i\eta\left(\partial_\xi - \frac{\xi}{2}\right) & \frac{\Delta}{2} - \omega_+\left(\frac{\xi^2}{4} - \partial_\xi^2\right) \end{pmatrix}$$

$$\xi = \frac{\sqrt{2}}{\ell_B}(y - k_x\ell_B^2) \qquad \omega_\pm = 2\frac{D \pm B}{\ell_B^2}$$

Two functions to the Weber equation:

$$\left(\frac{d^2}{d\xi^2} - \frac{\xi^2}{4}\right)y(\xi) = \lambda y(\xi)$$

$$\left(\partial_\xi - \frac{1}{2}\xi\right)U_\lambda(\xi) = -U_{\lambda-1}(\xi),$$
$$\left(\partial_\xi + \frac{1}{2}\xi\right)U_\lambda(\xi) = -\left(\lambda + \frac{1}{2}\right)U_{\lambda+1}(\xi),$$
$$\left(\partial_\xi - \frac{1}{2}\xi\right)V_\lambda(\xi) = \left(\lambda - \frac{1}{2}\right)V_{\lambda-1}(\xi),$$
$$\left(\partial_\xi + \frac{1}{2}\xi\right)V_\lambda(\xi) = V_{\lambda+1}(\xi).$$

$$\varphi_u(\xi) = \begin{pmatrix} u_1 U_\lambda(\xi) \\ u_2 U_{\lambda-1}(\xi) \\ u_3 U_\lambda(\xi) \\ u_4 U_{\lambda-1}(\xi) \end{pmatrix}$$

$$\varphi_v(\xi) = \begin{pmatrix} v_1 V_\lambda(\xi) \\ v_2 V_{\lambda-1}(\xi) \\ v_3 V_\lambda(\xi) \\ v_4 V_{\lambda-1}(\xi) \end{pmatrix}$$

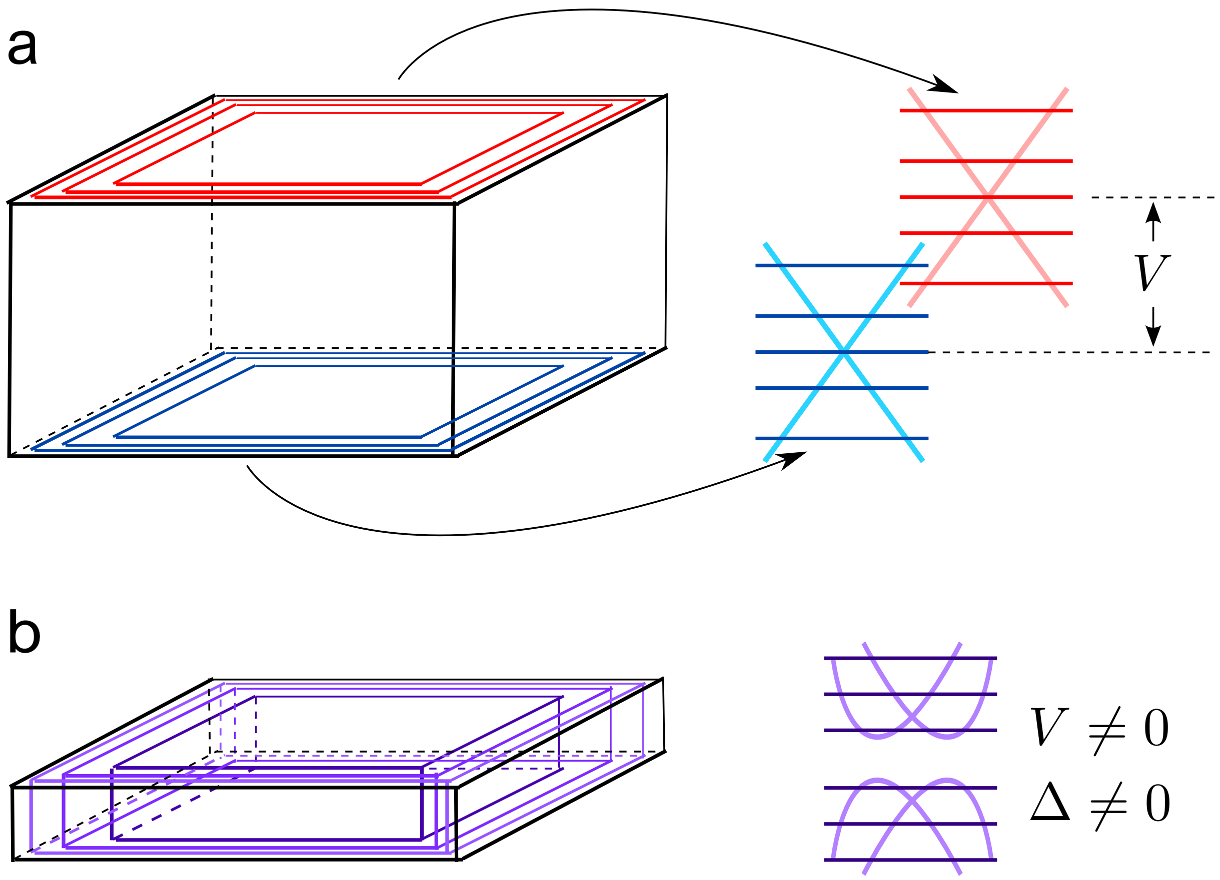
a
V
b
$V \neq 0$
$\Delta \neq 0$

Two patterns of QHE

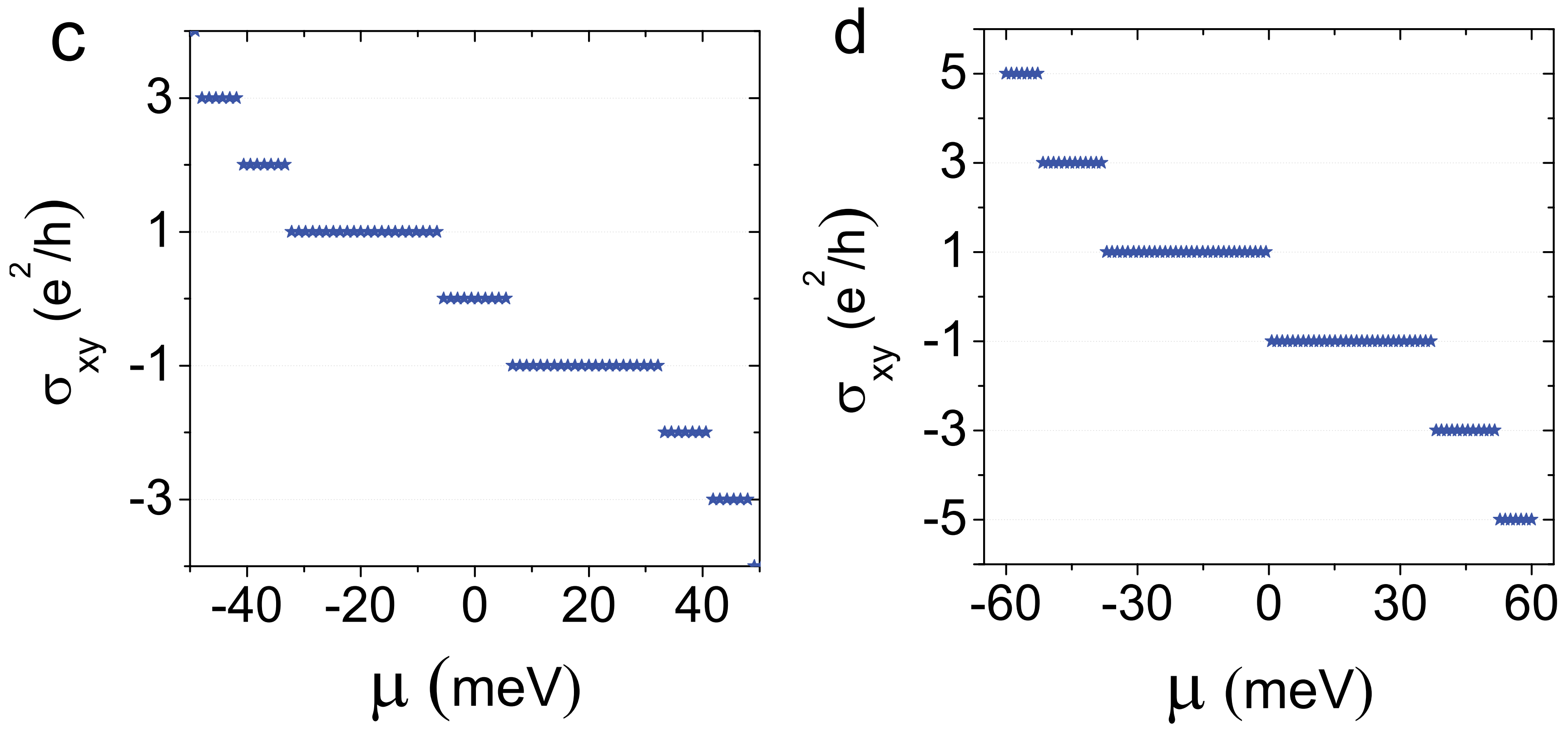

Landau Levels and Edge States

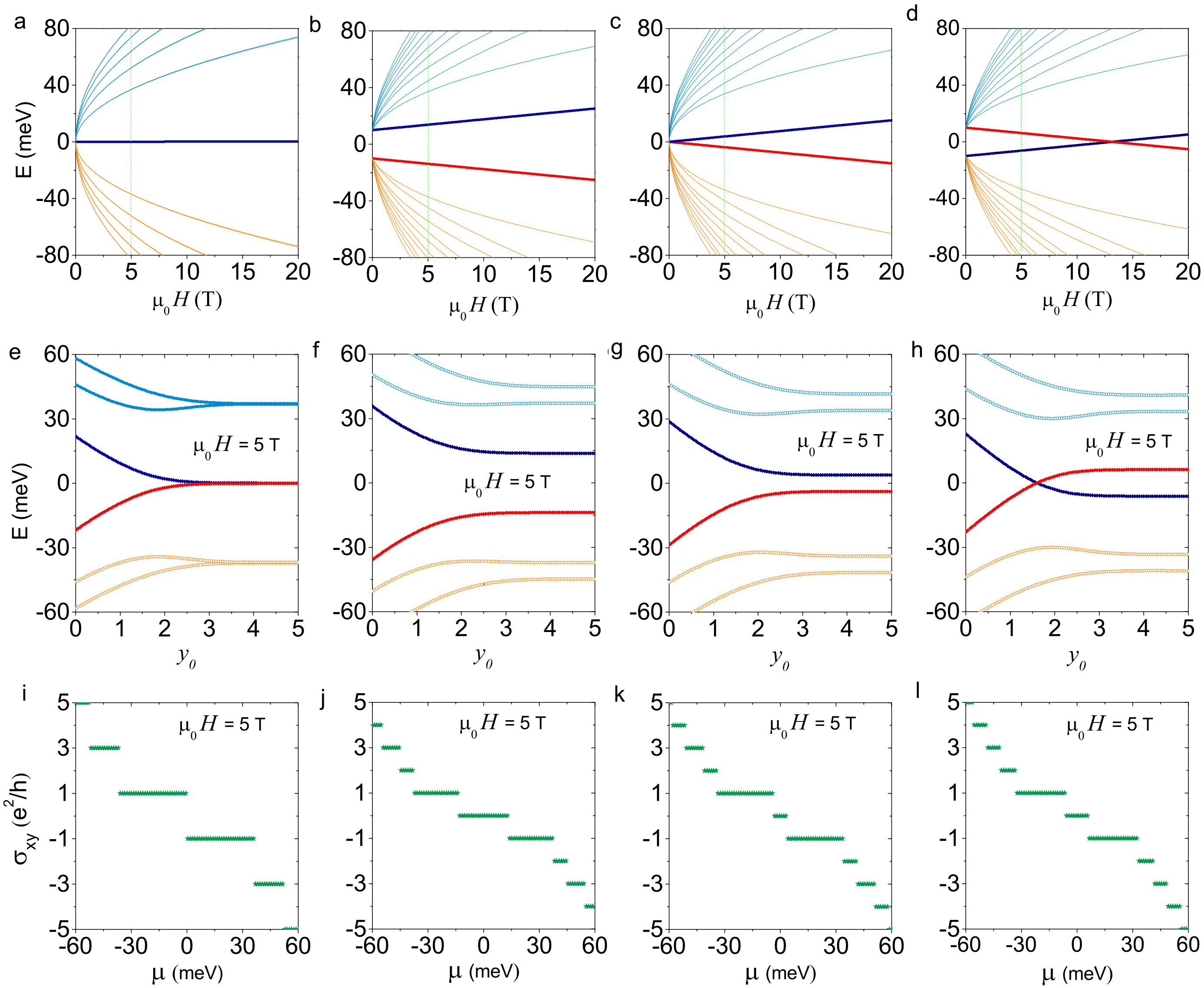

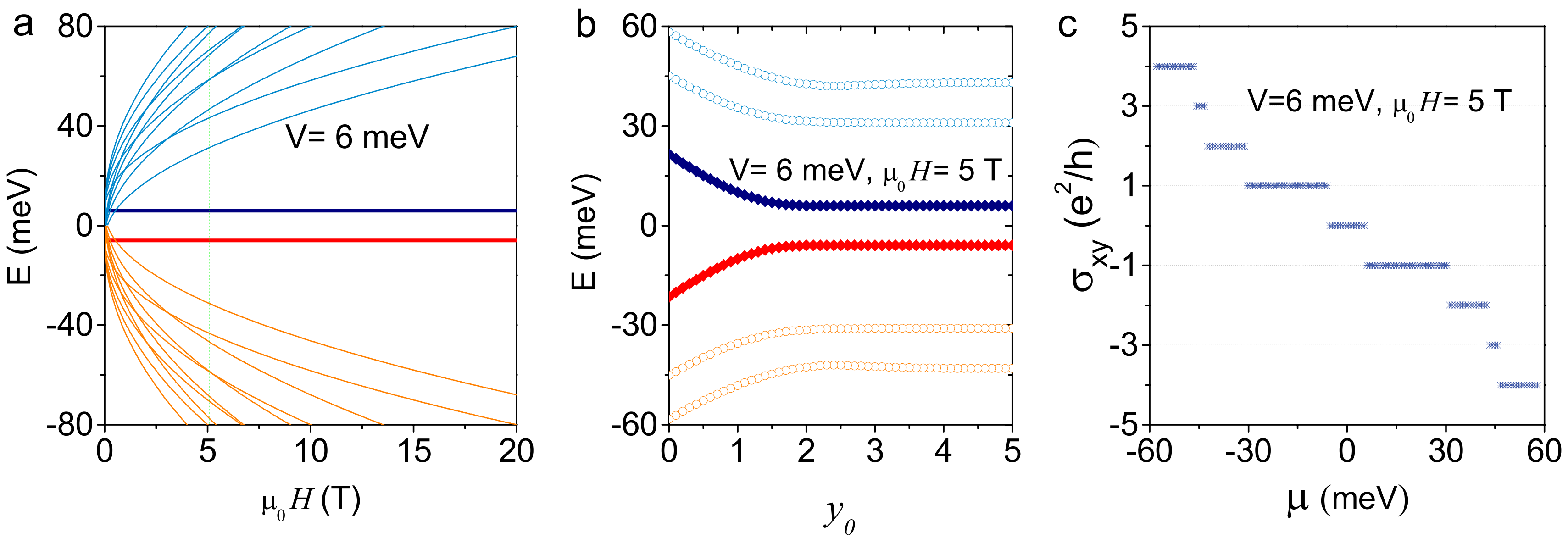

FIG. 3: **Integer quantized Hall plateaux due to SIA**. For case (i) with $\Delta = 0$ and $B \to 0$ but a finite $V = 6$ meV, (a) the fan diagram, (b) the energies of the two LLs of $n = 0$ near the edge, and (c) the Hall conductance as a function of the chemical potential μ. SIA breaks the degeneracies of all LLs in the thick film where $\Delta = 0$ and $B \to 0$. As a result, even integer Hall conductance plateaux also appear.

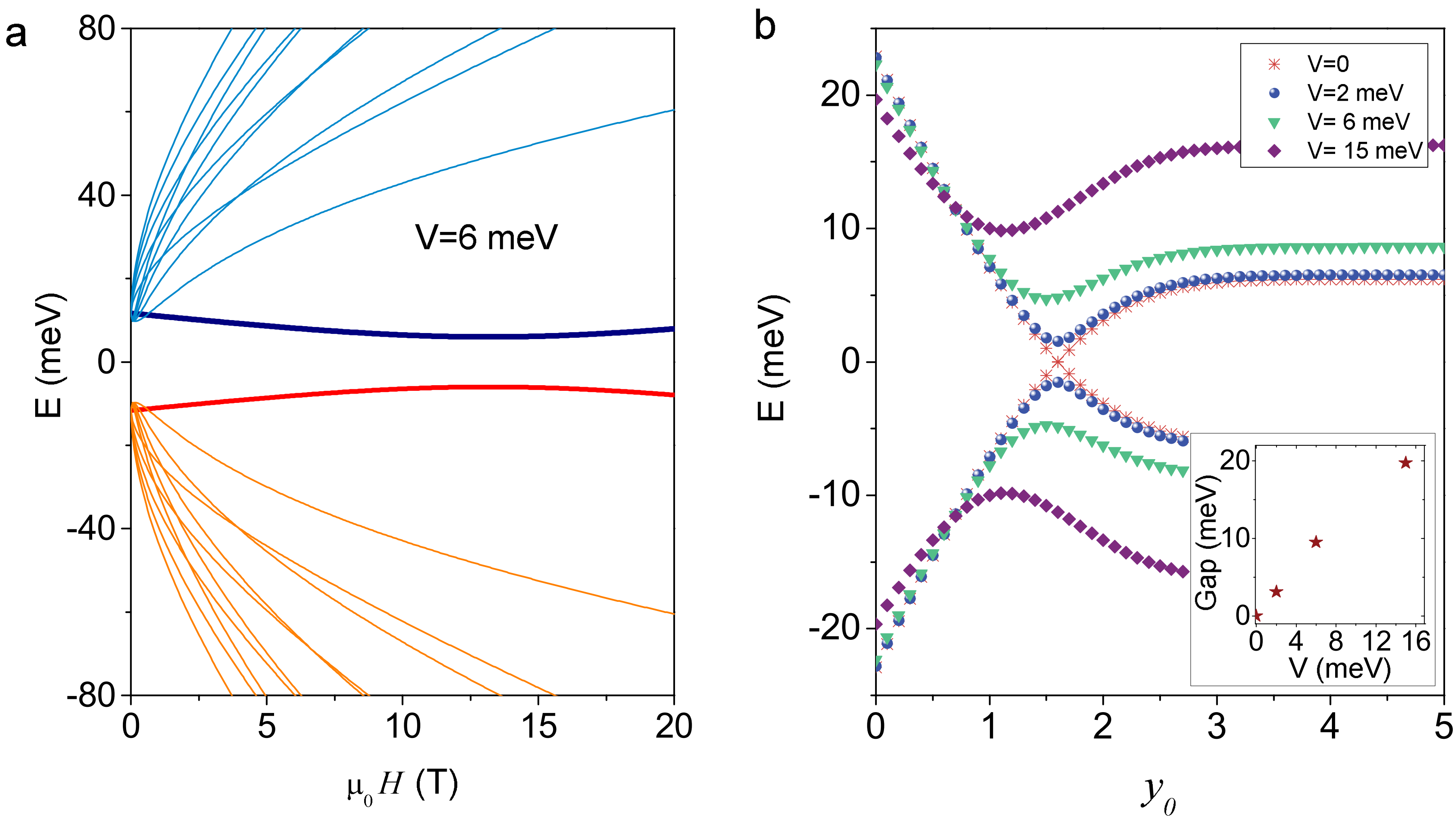

FIG. 4: **SIA-induced breakdown of the quantum spin Hall phase.** (a) The fan diagram in the presence of SIA, i.e., $V \neq 0$. SIA turns the crossing between the two LLs of $n = 0$ in Fig. 2d into an anti-crossing. (b) The energies of the two LLs of $n = 0$ at 5 T near the edge for different V. In the presence of SIA, the two LLs do not cross near the edge and open an energy gap. Inset: the gap opened between the two LLs of $n = 0$ as a function of V. The parameters are $\gamma = 300$ meVnm, $\Delta = -20$ meV, and $B = -500$ meVnm^2.

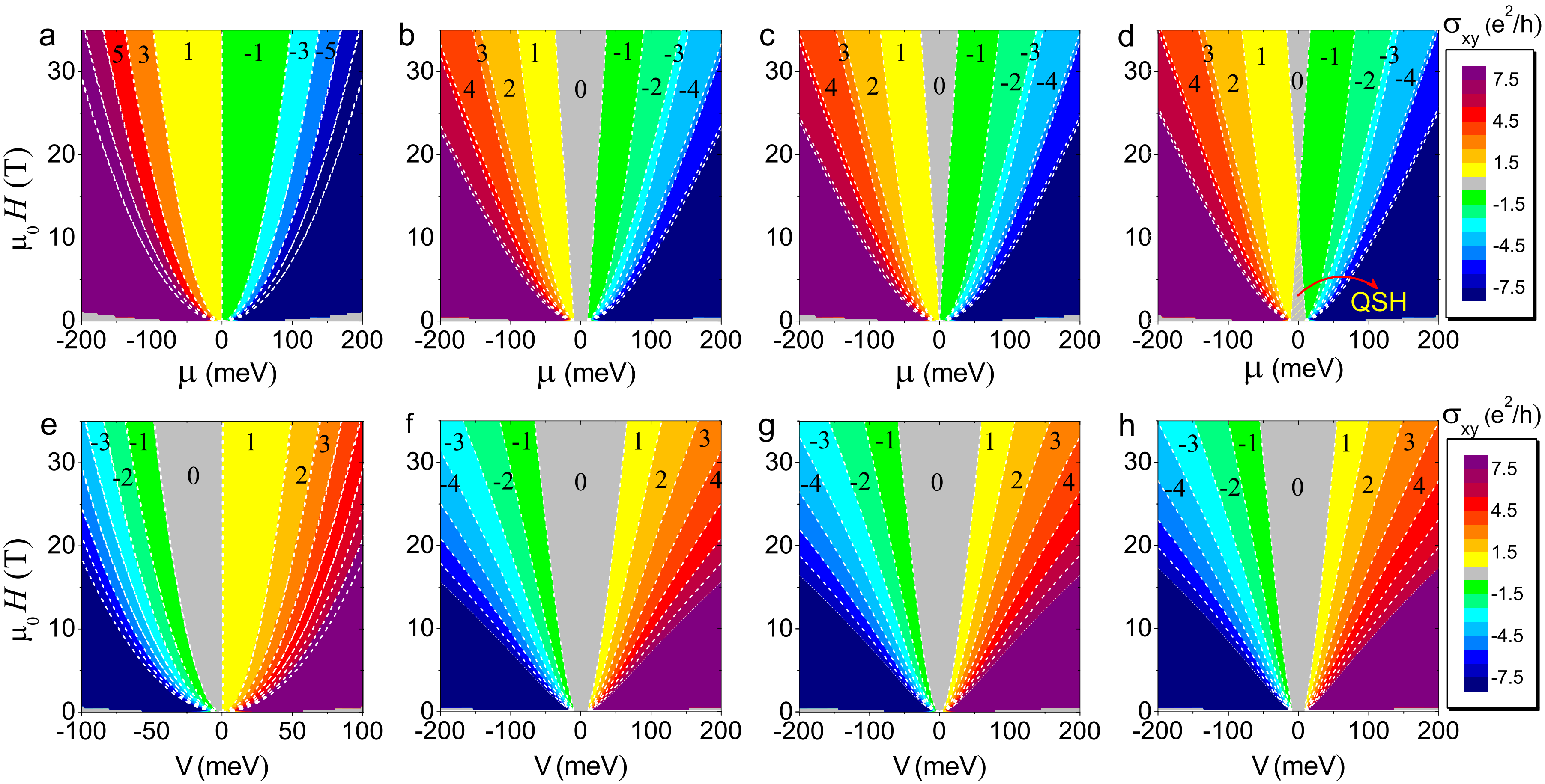

FIG. 5: **Phase diagrams of the quantum Hall effect in topological insulator films.** (a-d) The phase diagrams as functions of the chemical potential μ and magnetic field $\mu_0 H$ in the absence of SIA , i.e., $V = 0$. Different phases are denoted by corresponding Hall conductance σ_{xy} in units of e^2/h. The white dotted lines are the boundaries between different phases. The four columns compare cases with different finite size gap Δ and B. From left to right, (i) $\Delta = 0$ and $B \to 0$; (ii) $\Delta B < 0$; (iii) $\Delta = 0$ and $B \neq 0$; (iv) $\Delta B > 0$. The parameters for different cases are the same as those in Fig. 2. σ_{xy} is antisymmetric with respect to μ. In (a), there are only odd integer quantum Hall phases. In (b-d), there are both odd and even integer quantum Hall phases. In (d), the quantum spin Hall (QSH) phase is marked. (e-h) The phase diagrams as functions of V and $\mu_0 H$ while fixing the chemical potential $\mu = -V - 0^+$. Both odd and even integer quantum Hall phases can be induced by changing V in all the four cases.

Integer Quantized Hall Conductance

Lu, Shan, Chu, Niu & Shen, PRB 81, 115407(10)

$$H = v_F \hbar k \cdot \sigma + (m v_F^2 - B k^2) \sigma_z$$

$$\sigma_H = -\frac{e^2}{2h}\left[\mathrm{sgn}(m) + \mathrm{sgn}(B)\right]$$

The Hall Conductance and the Chern Number

The system Hamiltonian

Thouless, Kohmoto*, Nightingale, and den Nijs, **Phys. Rev. Lett. 49, 405(1982)**

$$H = \epsilon(p) + \sum_{\alpha=x,y,z} d_\alpha(p)\sigma_\alpha$$

The Kubo formula for the conductance: a result of linear response theory

$$\sigma_{ij} = \frac{e^2\hbar}{\Omega} \sum_{p,\mu\neq\mu'} \frac{(f_{p\mu} - f_{p\mu'})\mathrm{Im}(\langle p\mu|v_i|p\mu'\rangle\langle p\mu'|v_j|p\mu\rangle)}{(E_{p\mu} - E_{p\mu'})(E_{p\mu} - E_{p\mu'} + i\delta^+)}$$

$$\sigma_{ij} = -\frac{e^2\hbar}{2\Omega}\sum_p \frac{(f_{p,-} - f_{p,+})}{d^3} \epsilon_{\alpha\beta\gamma} \frac{\partial d_\alpha}{\partial p_i}\frac{\partial d_\beta}{\partial p_j} d_\gamma.$$

$$\sigma_H = \nu \frac{e^2}{h}$$

Hall conductance

The Chern number is an integer if the Brillouin zone is finite.

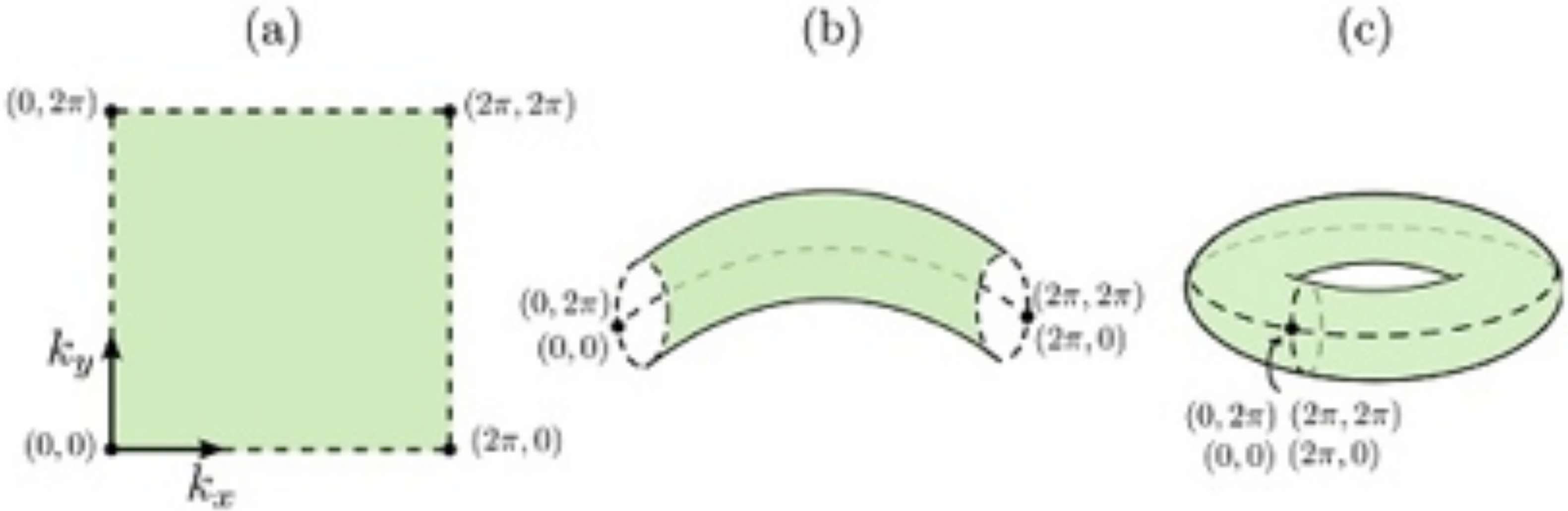

Equivalence of the first Brillouin zone and a torus: (a). A rectangle of the first Brillouin zone with periodic boundary conditions (b). The rectangle is rolled into a tube along the ky direction. (c). The tube is rolled into a torus along the kx direction. The four corners of the rectangle are actually the one point in the torus surface.

The edge states of n=0 Landau level for different coefficient B.

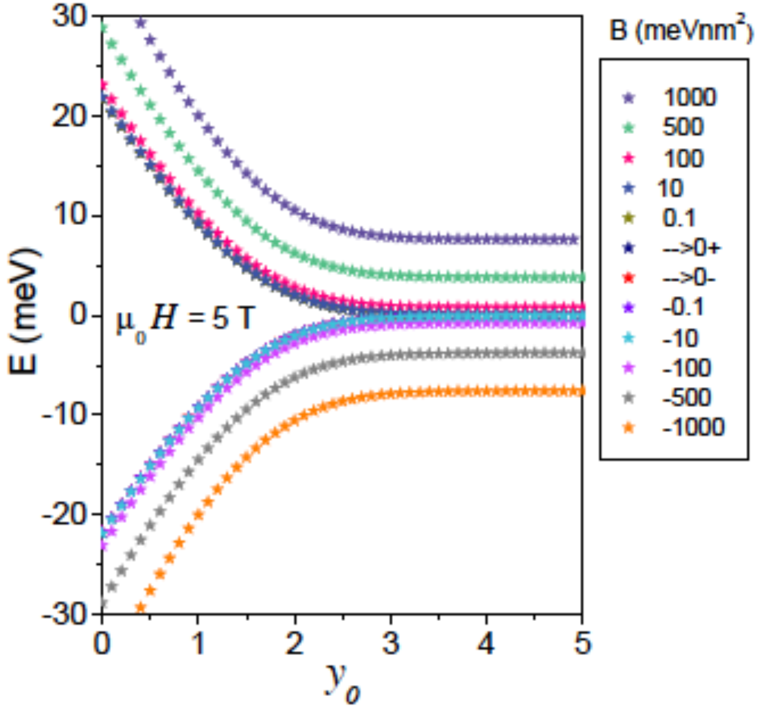

$$H = \begin{pmatrix} \frac{\Delta}{2} - B\left(k_x^2 + k_y^2\right) & \gamma\left(k_y + ik_x\right) \\ \gamma\left(k_y - ik_x\right) & -\frac{\Delta}{2} + B\left(k_x^2 + k_y^2\right) \end{pmatrix}$$

$$\frac{E}{|\eta|} = \mathrm{sgn}(B)\frac{U_{\lambda_- - 1}(\xi_0)}{U_{\lambda_-}(\xi_0)}$$

$$\eta = \sqrt{2}\gamma/\ell_B$$

Summary

- We established a model for topological insulator thin film.
- We find a solution of topological insulator thin film in a B field.
- We discussed the edge state effect.

Spin-Orbit Coupling: Semi-classical picture

Spin-Orbit Interaction (LS coupling): The interaction describes the effect of an electron's orbital motion on the orientation of its spin.

$$B = \left(\frac{\mu_0}{4\pi}\right)\frac{j\times r}{r^3} = -\frac{1}{ec^2 r}\frac{\partial V}{\partial r}(v\times r) = \frac{1}{emc^2}\frac{1}{r}\frac{\partial V}{\partial r}L$$

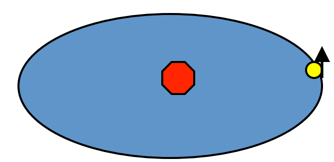

The potential energy of spin moment in this field is

$$U = -\mu_s\cdot B = g\frac{\mu_B}{emc^2\hbar}\frac{1}{r}\frac{\partial V}{\partial r}L\cdot S = \frac{1}{m^2c^2}\frac{1}{r}\frac{\partial V}{\partial r}L\cdot S$$

Spin transverse force (Shen 05):

$$F_f = \frac{e^2|E|}{4m^2c^4}J_S^E\times E$$

Spin Current

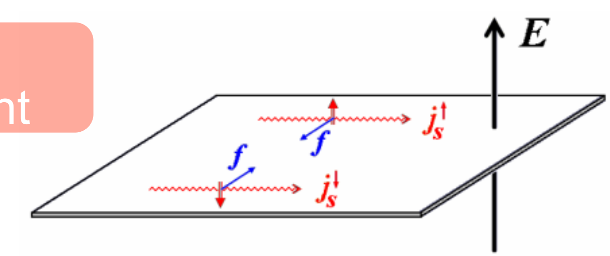

Half-Quantized Hall Conductance in Graphene?

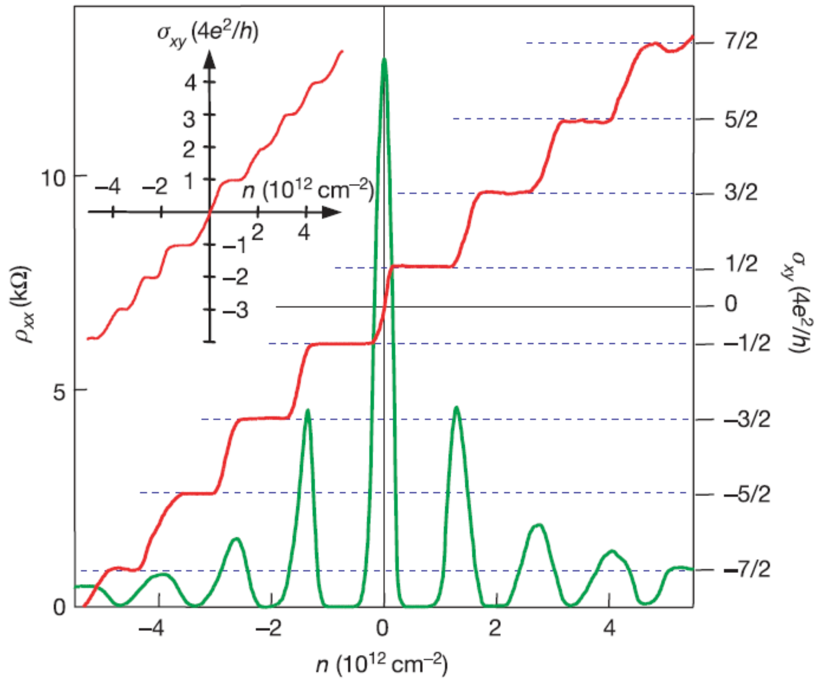

Figure 4 | QHE for massless Dirac fermions. Hall conductivity σ_{xy} and longitudinal resistivity ρ_{xx} of graphene as a function of their concentration at $B = 14$ T and $T = 4$ K. $\sigma_{xy} \equiv (4e^2/h)\nu$ is calculated from the measured dependences of $\rho_{xy}(V_g)$ and $\rho_{xx}(V_g)$ as $\sigma_{xy} = \rho_{xy}/(\rho_{xy}^2 + \rho_{xx}^2)$. The behaviour of $1/\rho_{xy}$ is similar but exhibits a discontinuity at $V_g \approx 0$, which is avoided by plotting σ_{xy}. Inset: σ_{xy} in 'two-layer graphene' where the quantization sequence is normal and occurs at integer ν. The latter shows that the half-integer QHE is exclusive to 'ideal' graphene.

Two valleys +
Double spin degeneracy

$$\sigma_H = (n + 1/2)\frac{4e^2}{\hbar}$$

$$= (4n + 2)\frac{e^2}{\hbar}$$

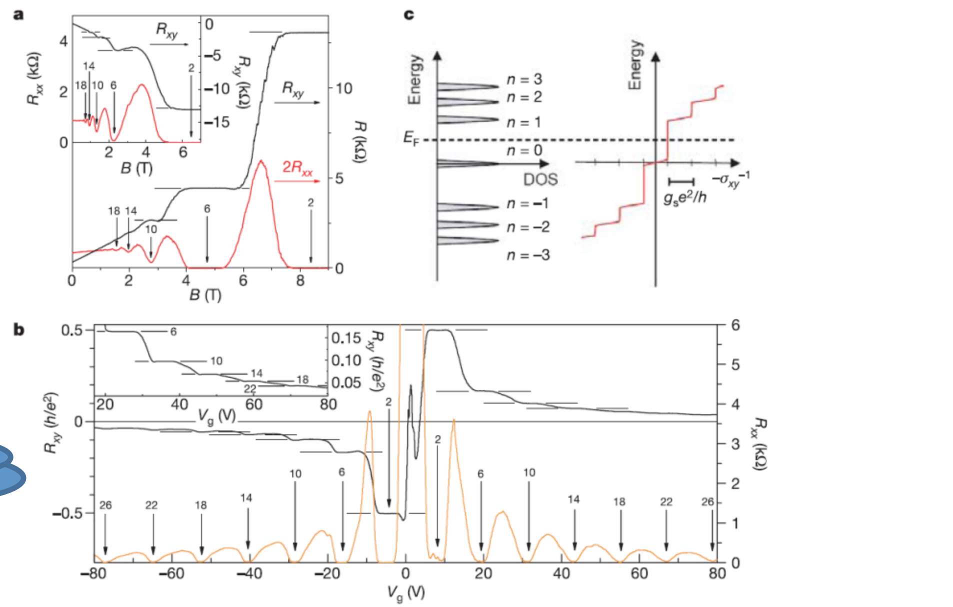

Figure 2 | Quantized magnetoresistance and Hall resistance of a graphene device. a, Hall resistance (black) and magnetoresistance (red) measured in the device in Fig. 1 at $T = 30$ mK and $V_g = 15$ V. The vertical arrows and the numbers on them indicate the values of B and the corresponding filling factor ν of the quantum Hall states. The horizontal lines correspond to $h/e^2\nu$ values. The QHE in the electron gas is shown by at least two quantized plateaux in R_{xy}, with vanishing R_{xx} in the corresponding magnetic field regime. The inset shows the QHE for a hole gas at $V_g = -4$ V, measured at 1.6 K. The quantized plateau for filling factor $\nu = 2$ is well defined, and the second and third plateaux with $\nu = 6$ and $\nu = 10$ are also resolved. **b**, Hall resistance (black) and magnetoresistance (orange) as a function of gate voltage at fixed magnetic field $B = 9$ T, measured at 1.6 K. The same convention as in **a** is used here. The upper inset shows a detailed view of high-filling-factor plateaux measured at 30 mK. **c**, A schematic diagram of the Landau level density of states (DOS) and corresponding quantum Hall conductance (σ_{xy}) as a function of energy. Note that, in the quantum Hall states, $\sigma_{xy} = -R_{xy}^{-1}$. The LL index n is shown next to the DOS peak. In our experiment the Fermi energy E_F can be adjusted by the gate voltage, and R_{xy}^{-1} changes by an amount $g_s e^2/h$ as E_F crosses a LL.

Zhang et al, Nature 438, 201 (2005)

Band Structure of Graphene in B field

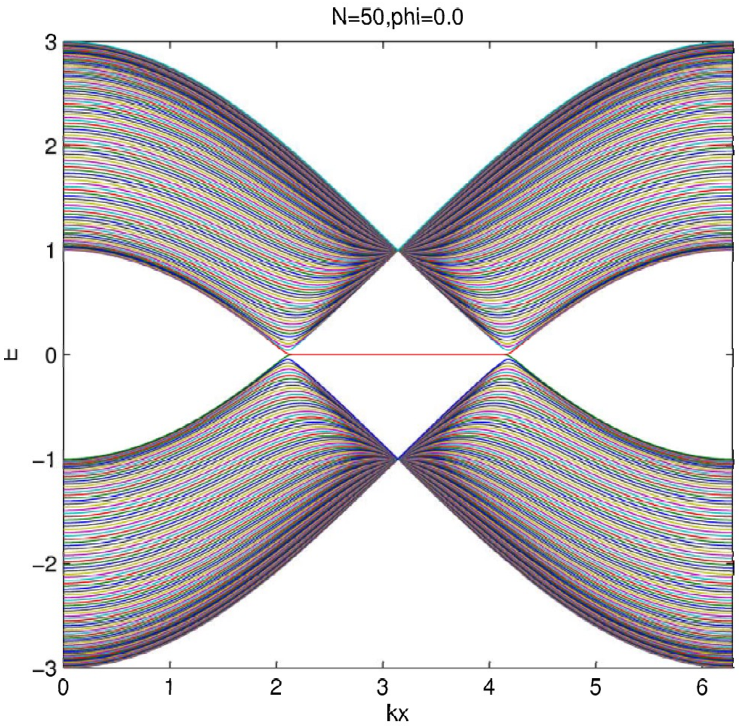

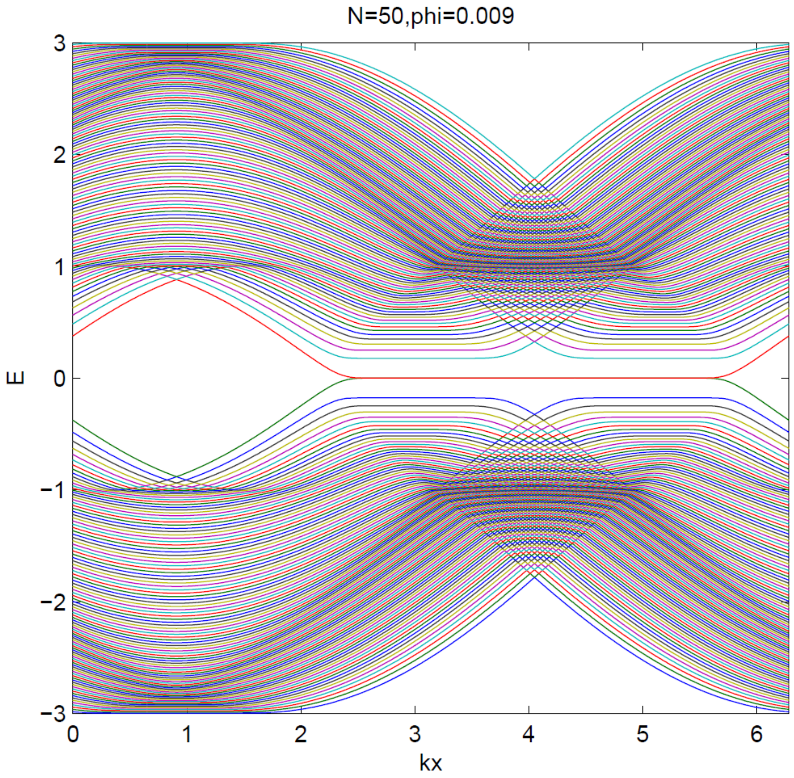

The zero mode edge states connects two valleys. So the zero-mode conductance originates from the one edge state connecting two valleys, NOT from two one-halfs of two valleys

QAHE & Edge State

Surface States in a Zeeman Field

Chu, Shi and Shen, 2011

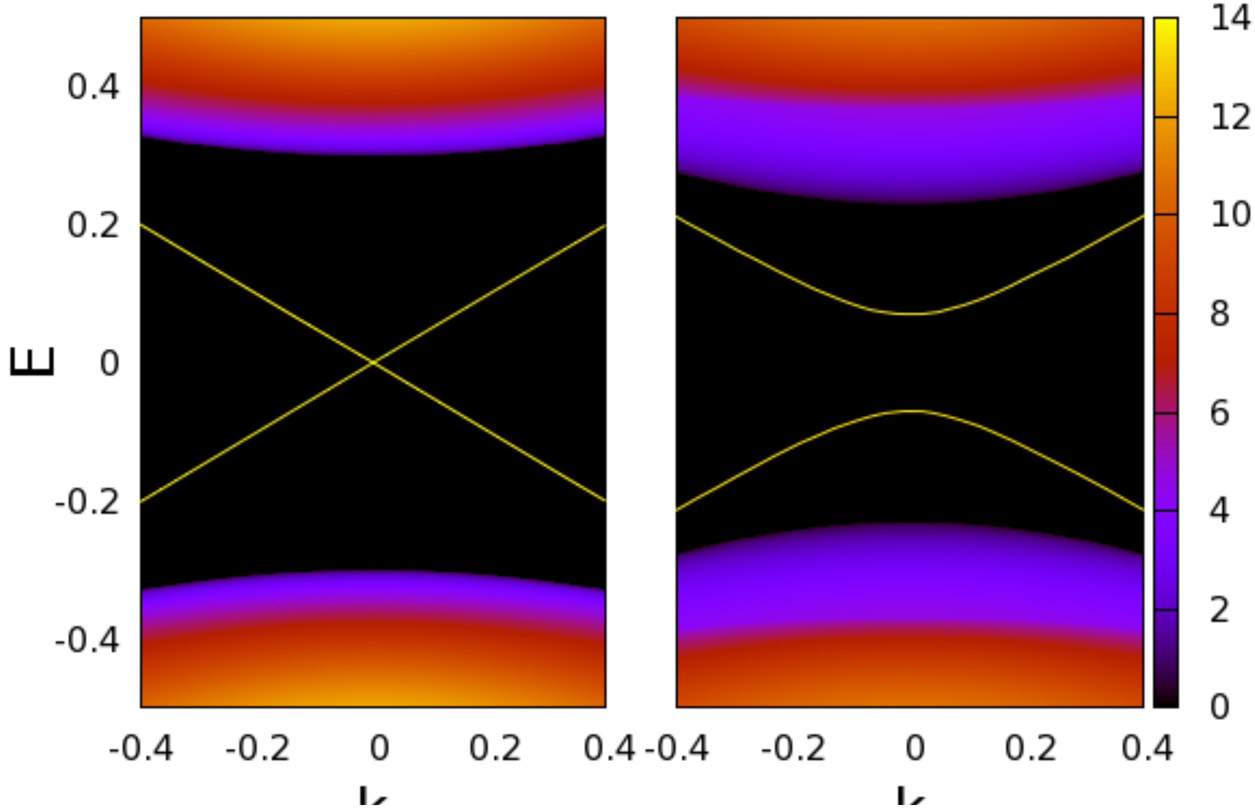

FIG. 2: (Color online) Local density of state on an infinite xy surface of a semi-infinite 3D system. (left) gapless single Dirac cone of the surface state; (right) gap opening by application of a Zeeman splitting term. The model parameters are $A = 0.5$, $B = 0.25$, $M = 0.3$, and $\Delta_z = 0.07$.

Half-Quantized Hall Conductance for Two Dimensional Massive Dirac Gas

Redlich, PRD 29, 2366(84); Jackiw, PRD 29, 2375(84)
Qi et al, PRB (2008),Chu et al, PRB(2011)

$$H = v_F \hbar k \cdot \sigma + m v_F^2 \sigma_z = d \cdot \sigma$$

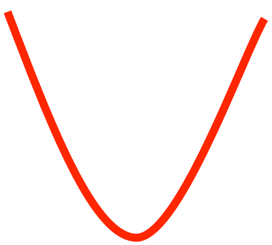

$$\sigma_H = -\frac{e^2}{2h} \sum_k \frac{d \cdot (\partial_{k_x} d \times \partial_{k_y} d)}{d^3}$$

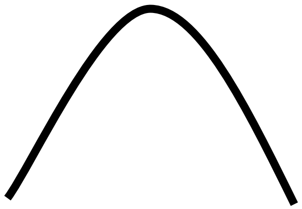

$$\sigma_H = -\frac{e^2}{2h} \mathrm{sgn}(m)$$

Half-Quantization in B-field

$$H = v_F p \cdot \sigma \rightarrow v_F (p - \frac{e}{c} A) \cdot \sigma$$

$$H = v_F \begin{pmatrix} 0 & \Pi_- \\ \Pi_+ & 0 \end{pmatrix} = \sqrt{2}\,\frac{\hbar v_F}{l_B} \begin{pmatrix} 0 & a \\ a^+ & 0 \end{pmatrix}$$

$$E_n = \pm\sqrt{n\hbar eB};\left|n,\pm\right\rangle = \frac{1}{\sqrt{2}} \begin{pmatrix} \left|n-1\right\rangle \\ \pm\left|n\right\rangle \end{pmatrix}$$

$$E_{n=0} = 0;\left|n=0\right\rangle = \begin{pmatrix} 0 \\ \left|0\right\rangle \end{pmatrix}$$

$$\boxed{\sigma_H = (n + 1/2)\frac{e^2}{h}}$$